Magnetohydrodynamic Turbulent Fluid Flow past an Infinite Vertical Porous Plate in a Rotating System

Job Oqhoyho Mayaka

MC300–0004/2012

A thesis submitted to The Pan African University Institute for Basic Sciences, Technology and Innovation in partial fulfilment of the requirements for the degree of Master of Science in Mathematics (Computational option).

2014

Declaration

I declare that this thesis is my own work and has not been submitted in any university or other institution for the award of a degree or any other award.

Student's name: Job Oqhoyho Mayaka

Signature: _____ **Date:** .....

The student, named above, worked under our supervision and the work reported in this thesis is his own work.

Supervisor's name: Professor Mathew Kinyanjui
Director, Board of Postgraduate Studies
Jomo Kenyatta University of Agriculture and Technology
P.O. Box 62000 – 00200
NAIROBI

Signature: _____ **Date:** .....

Supervisor's name: Professor Johana Sigey
Director, Kisii CBD Campus
Jomo Kenyatta University of Agriculture and Technology
P.O. Box 62000 – 00200
NAIROBI

Signature: _____ **Date:** .....

Dedication

To my daughter, Luvynnah.

Acknowledgement

I wish to acknowledge my professor and supervisor, Professor Mathew Kinyanjui, for his superior guidance leading to this study. I also extend my regards to my second supervisor, Professor Johana Sigey, for sharing with me his knowledge and assisting me in the understanding of the problem and its development. In the same vein, I thank my lecturers for their selflessness in sharing knowledge, some of which I have used in writing this thesis.

I also thank my family, especially my wife, Medrine, and daughter, Luvynnah for their patience during the pursuit of my studies. They understood the pressures of being a student and bore with me during the entire time I have been pursuing the course.

Further, my regards go to my colleagues, the pioneer students at PAUISTI, for the many informative discussions we have held. More so, my regards are due to my classmates, Dawit and Samuel.

Last, let me extend my regards to the Pan African University for offering me the scholarship to undertake this course. I surely could not have pursued this course without the scholarship. Thank you all.

TABLE OF CONTENTS

Nomenclature

Roman Symbols

Symbols	Quantity
J	Current density, A/m^2
J_x, J_z	Current density, A/m^2 in the x and z direction
H, B	Magnetic field intensity, Wb/m^2
M	Mass, kg
E	Electric field, V/m
u, v, w	Components of velocity in the x, y and z directions, respectively, m/s
P	Pressure of the fluid, N/m^2
P_e	The electron pressure, N/m^2
F_μ	Viscous force, N
e	Electronic charge, C
g	Acceleration due to gravity, m/s^2
H_0	Constant magnetic field intensity, Wb/m^2
k	Thermal conductivity, $W/m/K$
l	Characteristic length
T	Absolute temperature
C_p	Specific heat at constant pressure, $J/kg/K$
U^*, V^*, W^*	Dimensional mean velocity components, m/s
x^*, y^*, z^*	Dimensional Cartesian co-ordinates
t^*	Dimensional time, s
T^*	Dimensional temperature, K
T_∞^*	Temperature of the fluid in the free stream, K
T_w^*	Temperature of the fluid at the plate, K
C^*	Dimensional concentration, mol/m^3
C_∞^*	Concentration of the fluid in the free stream, mol/m^3
C_w^*	Concentration of the fluid at the plate, mol/m^3
$\mathscr{V}$	Volume, m^3
$\mathscr{C}$	Arbitrary constant
U, V, W	Dimensionless mean velocity components
x, y, z	Dimensionless Cartesian co-ordinates
t	Dimensionless time
C	Dimensionless concentration
q	Electric charge, C
Re_{cr}	Critical Reynold's number
Gr_L	Thermal variant of Grashof number
Sc	Schmidt number
M^2	Magnetic parameter
Ec	Eckert number

m	Hall parameter ($\omega_e \tau_e$)
Pr	Prandtl number
Er	Rotational parameter
v_0	Dimensionless injection or suction velocity
n	Number of charged particles

Greek Symbols

Symbols	**Quantity**
ρ	Fluid density, kg/m^3
ρ_q	Volumetric charge density, C/m^3
ρ_0, ρ_∞	Reference and free stream fluid densities, kg/m^3
μ	Coefficient of viscosity, kg/ms
μ_0	Magnetic permeability, H/m
$\Delta t, \Delta z$	Time and distance intervals
υ	Kinematic viscosity, m^2/s
τ_e	Collision time of electrons, s
β	Coefficient of thermal expansion, K^{-1}
β_C	Coefficient of concentration expansion, mol^{-1}
σ	Electrical conductivity, $\Omega^{-1}m^{-1}$
θ	Dimensionless fluid temperature
ω_e, ω_i	Electronic and ionic cyclotron frequency, Hz
τ_e, τ_i	Electronic and ionic cyclotron period, s
Ω	Rotational angular velocity, $rads^{-1}$
κ	von Karman constant
Π	Stress tensor
ζ	Arbitrary flow variable
ϕ, ς	Arbitrary functions
ϑ	Arbitrary independent variable

List of Abbreviations and Acronyms

MHD	Magnetohydrodynamic
FDM	Finite difference method
L.H.S	Left hand side
R.H.S	Right hand side
FTCS	Forward time central space
BTCS	Backward time central space

List of Figures

Abstract

In this study, the turbulent fluid flow problem of a conducting fluid past an infinite porous vertical plate in a rotating system is investigated. Hall currents, mass transfer and Joule's heating are accounted for in the present study. A deviation from the laminar flow, non–porous medium, Hall currents and Joule's heating is sought. Mathematical formulation in which turbulence is approximated using Prandtl mixing hypothesis is constructed. The final set of partial differential equations obtained is resolved into difference equations using the forward time central space finite difference method. A computer program in matlab is used to iteratively solve the resultant difference equations. The solutions obtained are presented in form of graphs. The effect of various non–dimensional parameters on the flow profiles are discussed and physical interpretation given. Mass transfer, rotation, Hall currents and Joule's heating are found to have profound effect on the primary velocities, secondary velocities, temperature and concentration profiles. The rotational parameter and Hall parameter are found to inhibit the primary velocities while enhancing the secondary velocities. Injection enhances all the flow variables while suction inhibits all flow variables. Results reported in the present study follow expected trends and are in good agreement with some of the previous studies.

CHAPTER ONE

INTRODUCTION

1.1 Background Information

A fluid is a substance that resists an applied compressive stress, but continually deforms (or flows) under an applied shear stress, regardless of the magnitude of the applied stress. Magnetohydrodynamics (MHD) is the study of the low frequency interaction between electrically conducting fluids and magnetic fields (Schnack, 2009). In such models it is assumed that the Maxwell displacement current is neglected and the fluid is treated as a continuum (Calvert, 2002).

The MHD problem is of great interest in current trends in mathematical modelling. This is due to its many applications in engineering problems e.g. MHD generators, plasma studies, nuclear reactors, oil exploration, geothermal extraction and boundary layer control in the field of aerodynamics.

MHD essentially involves the motion of an ionised fluid in a magnetic field. This leads to an inclusion of the Lorentz force in the equation of motion. A solution for the MHD problem in which mass, heat, velocity and concentration are transferred past a porous plate in a rotating system is sought. In the present study the problem is introduced, relevant literature reviewed, a mathematical model formulated for the problem, the arising partial differential equations numerically solved and the results obtained discussed.

1.2 The Geometry of the Problem

The current problem is that of a turbulent flow past an infinite vertical porous plate in a rotating system. Letting the vertical plate be in the $x - z$ plane, a strong constant magnetic field, H_0, is applied along the $y -$ axis as shown in Figure 1. 1 below.

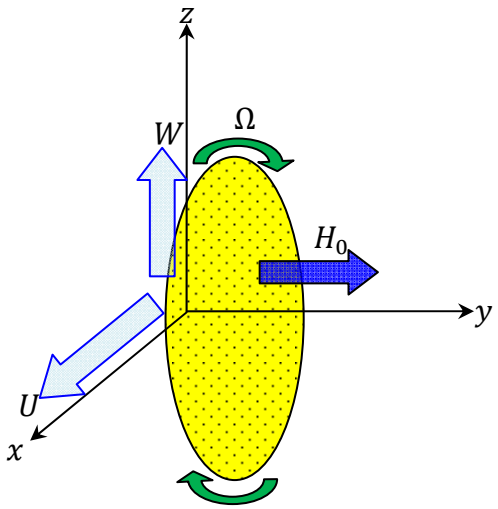

Figure 1. 1: A diagrammatic representation of the MHD flow problem

It is assumed that initially the plate and the fluid are in a rigid body rotation with constant angular velocity, Ω, about the $y - axis$.

1.3 The Physics of the Problem

1.3.1 Electromagnetic Induction

According to Faraday's law of electromagnetic induction, a conductor moving in a magnetic field will have an electric current induced in it (Serway and Jewett, 2004). Further, the induced current is maximised when the direction of motion is perpendicular to the applied magnetic field.

In a similar manner, if an ionised fluid flows through a magnetic field, then current is induced in the fluid. The current radiating per unit area is called the current density, $\boldsymbol{J}$. The force due to the interaction of the magnetic and electric fields is called Lorentz force.

1.3.2 The Hall Effect

Hall Effect is a phenomenon observed when a body of free charged particles is in a magnetic field. As per this phenomenon, there is a redistribution of charges in the body so as to set up a potential difference across its cross-section.

Since the fluid in question is moving in the $x-$ and $y-$ plane, the ions and electrons in the fluid will experience Hall Effect just like that experienced by the body. The redistribution of charges, according to Lenz's law of electromagnetism, will be in opposition of the fluid motion. The effect then will be to retard the motion. The kinetic energy of the particles reduces and this energy is dissipated as heat.

1.4 Statement of the problem

A study of the effect of various fluid parameters on the flow variables of MHD turbulent flow past an infinite vertical porous plate in a rotating system is carried out. The fact that the plate is porous implies that there will be diffusion of the fluid (mass transfer) across the plate. This will depend on concentration gradient leading to either injection or suction. An extension of the work of Mutua *et al* (2013) by considering the porosity of the plate or the work of Das *et al* (2011) but in a rotating system is sought.

An approximate solution to the problem using the forward time central space (FTCS) finite difference method (FDM) is obtained. The velocity (primary and

secondary), temperature and concentration profiles is obtained as variables of time (t) and space (y). A comparison between the present results and the theoretical results of Das *et al* (2011) and Mutua *et al* (2013) is carried out.

1.5 Objectives of the Study

1.5.1 General Objective

- To investigate the effect of the Hall currents, Joule's heating, mass transfer and heat transfer on the MHD turbulent flow past an infinite vertical porous plate in a rotating system.

1.5.2 Specific Objectives

(i) To mathematically develop the final set of governing partial differential equations for the MHD problem from the physical laws of hydrodynamics and electromagnetism.

(ii) To solve the final set of governing partial differential equations numerically using a computer program.

(iii) To determine the effect of the fluid properties (e.g. Prandtl number, Hall parameter, Schmidt number and rotational parameter) on the flow variables.

1.6 Justification

It is difficult to fully explain many physical phenomena. Even when an explanation exists, the mathematical prediction may not be exact since there are many assumptions. In most MHD studies, the assumption is that the flow is streamlined and laminar. In the current problem a deviation from this is sought as turbulence is taken into account. We also take into account the porosity of the

plate as well as the effect of a rotating system. Further, the Hall currents and Joule's heating are factored into previous models to give a model which is closer to the physical phenomenon of MHD.

The fact that MHD borrows from the same principle as the electrical generators, there is hope that by further study of MHD problems a future source of electricity may be found. This is so because the world we live in is surrounded by fluids (air) that can be tapped into to generate electricity. Other applications of MHD are plasma studies, nuclear reactors, oil exploration, geothermal extraction and boundary layer control in the field of aerodynamics. Due to these applications the field of MHD is an active area of study. Reduction of the number of assumptions yields closer predictions to the physical phenomenon of MHD.

In the next chapter, relevant literature is reviewed and the current MHD fluid flow problem placed in context.

CHAPTER TWO

LITERATURE REVIEW

2.1 Overview

In this chapter, we review relevant literature with the intension of placing the current problem in its context. We start by reviewing some studies involving porous plates; we then proceed to review those studies done in view of rotating systems and finally place the current study in the context of these studies. By so doing, we shall be showing the gap we are trying to bridge.

2.2 Early Developments

The study of MHD may be traced back to 1832 when Faraday attempted to measure currents of the River Thames which he believed was due to the moving ions in the water and the earth's magnetic field. Following the disagreements between engineering experiments and mathematical theory, Prandtl (1904) introduced the very important theory of boundary layers. Theoretical predictions and experimental results have been in closer agreement following the boundary layer theory. Then there was Hartmann (1937) who besides engineering the Hartmann pump also developed the theory of mercury dynamics (Hg-dynamics). This revolved around the physics of mercury flow in a magnetic field. However greater advances in MHD theory came about after Alfven (1942) discovered the Alfven waves. MHD has since seen great developments in both theory and experiment. The MHD physical problem is still active and more theories are still emerging.

2.3 Studies Involving Porous Plates

Hasimoto (1957) initiated the studies involving MHD flow past porous plates when he studied boundary layer growth on a flat plate with uniform suction or injection. Later, Mansuti *et al* (1993) discussed the steady flow of a non–Newtonian fluid past a porous plate with suction or injection.

Sharma and Pareek (2002) explained the behaviour of steady free convective MHD flow past a vertical porous moving surface. Makinde *et al* (2003) also discussed the unsteady free convective flow with suction on an accelerating porous plate. Following this, Das *et al* (2007) investigated numerically the unsteady free convective flow past an accelerated vertical porous plate with suction and heat flux. More recently, Das *et al* (2011) studied the mass transfer effects on unsteady hydromagnetic convective flow past a vertical porous plate in a porous medium with heat source.

2.4 Studies Involving Rotating Systems

Gupta and Soundalgekar (1975) having found that previous studies failed to yield the correct asymptotic solution for velocity distributions, studied the hydromagnetic flow and heat transfer in an infinite plate past a rotating porous wall. Kinyanjui *et al* (1998) studied the Stokes problem of convective flow past a vertical infinite plate in a rotating fluid.

Later, Kwanza *et al* (2003) analyzed MHD Stokes free convection flow past an infinite vertical porous plate subjected to constant heat flux with ion slip current and radiation absorption. Chaudhary (2006) studied combined heat and mass transfer effects on MHD free convection flow past an oscillating plate imbedded in porous medium.

More recently, Ghosh and Ghosh (2008) studied the hydromagnetic rotating flow of a dusty fluid near a pulsating plate with several limiting case studies. Marigi *et al* (2012) analysed the hydromagnetic turbulent flow past a semi-infinite vertical plate subjected to heat flux. Mutua *et al* (2013) studied the Stokes problem of a free convective flow past a vertical infinite plate in a rotating fluid with Hall currents in the presence of a variable magnetic field.

2.5 Current Problem

Currently, a study of the MHD problem of a rotating fluid past a porous plate is carried out. The present problem takes into account a porous plate, Hall currents and Joule's heating, therefore, extending the work of Das *et al* (2011) but in a rotating system and the work of Mutua *et al* (2013) but taking into account a porous plate. The study is intended to investigate the effects of heat transfer, mass transfer and Joule's heating on velocity, temperature and concentration profiles of the suggested fluid flow problem.

In the next chapter we formulate a mathematical model corresponding to the MHD flow problem described in section 1.4.

CHAPTER THREE

GOVERNING EQUATIONS

3.1 Overview

In this chapter, a mathematical model for the physical problem described in section 1.4 is formulated. As many physical variables as are mathematically possible to solve are taken into account. However, many physical problems provide mathematical challenges and it is instructive to make some physically meaningful assumptions to reduce the problem into a solvable one. The general equations are first developed, these equations are then reduced by making assumptions, non-dimensional parameters are adopted into the equations to reduce them even further and finally turbulence and porosity are introduced. This yields the final set of governing equations for the model.

3.2 Assumptions and Approximations

It is very difficult to describe a physical phenomenon like MHD mathematically. To arrive at the final governing equations several assumptions and approximations are made. Here is a summary of the most prominent of them:

(i) The ratio of the square of the fluid velocity V and that of the square of the velocity of light c is negligibly small i.e. $\left(\frac{V^2}{c^2} \ll 1\right)$.

(ii) The fluid is assumed to be incompressible hence the density of the fluid is assumed a constant of both time and space.

(iii) There is no chemical reaction taking place in the fluid.

(iv) A short circuit problem where no charges accumulate is considered. Thus electrostatic force, $\rho_e \mathbf{E}$, is negligible.

(v) The displacement current, $\boldsymbol{D}$, is negligible with respect to the electric current density, $\boldsymbol{J}$.

(vi) The plate is non-conducting.

(vii) The Magnetic Reynolds number is very large implying that magnetic diffusion is negligible.

(viii) The magnetic field is considered relatively strong and constant.

(ix) The ion–slip currents are negligible. The applied magnetic field is not sufficiently strong to cause appreciable ion–slip currents

(x) The stress tensor for the magnetohydrodynamic problem is approximated to its hydrodynamic analogue.

(xi) Turbulence in the flow is approximated using the Prandtl mixing hypothesis.

3.3 General Governing Equations

3.3.1 Equation of Continuity

The equation of continuity arises from the principal of conservation of mass. This requires that, under normal conditions mass can neither be created nor destroyed (Hughes and Gaylord, 1964).

Considering an infinitesimal fluid element of volume, $d\mathscr{V}$, the mass of the volume element, M, becomes:

$$M = \int \rho d\mathscr{V} \tag{3.3.1}$$

In the event that there are no sources or sinks of mass within the element, dV, $\frac{dM}{dt}$ is just the rate at which mass enters or leaves through the surfaces enclosing $d\mathscr{V}$. The mass flux through an infinitesimal surface element $d\mathbf{S}$ is $\rho\mathbf{V}$, where $\mathbf{V}$ is the velocity. This implies that the total rate of flow of mass out of the volume element is given by:

$$\frac{d}{dt}\int_V \rho d\mathscr{V} = -\oint_S \rho\mathbf{V}\cdot d\mathbf{S} \tag{3.3.2}$$

Using Gauss' theorem in the R.H.S of equation (3.3.2), one has:

$$\int_V \frac{\partial\rho}{\partial t} d\mathscr{V} = -\int_V \nabla\cdot(\rho\mathbf{V})\, d\mathscr{V} \tag{3.3.3}$$

Since equation (3.3.3) holds for all arbitrary infinitesimal volumes it can be simplified to:

$$\frac{\partial\rho}{\partial t} + \nabla\cdot(\rho\mathbf{V}) = 0 \tag{3.3.4}$$

Equation (3.3.4) is easily reduced by the assumption that the fluid is incompressible to become:

$$\nabla\cdot\mathbf{V} = 0 \tag{3.3.5}$$

3.3.2 Equation of motion

This is also known as the equation of momentum (Versteeg and Malalasekera, 2007). It relies on both Newton's second law of motion and the principle of conservation of momentum. Newton's second law of motion states that the rate of change of momentum is directly proportional to the net force causing the change and is in the direction of that resultant force. On the other hand the principle of

conservation of momentum requires that the total momentum remain the same when two or more bodies interact provided there is no external forces act. For a unit volume, this can be stated as:

$$\rho \frac{d\mathbf{V}}{dt} = \mathbf{F} \tag{3.3.6}$$

The net forces per unit volume are represented by letter $\mathbf{F}$ in Equation (3.3.6). These forces are classified into body forces and surface forces.

3.3.2.1 Body Forces

These are the forces that act throughout the body of a fluid element. They usually originate at a distance but affect the body's state of motion. In MHD, the body forces are the gravitational force and the electromagnetic forces. Both of these affect the present MHD problem.

3.3.2.1.1 Gravitational Force

Due to the geometry of the present problem the gravitational force will affect the flow properties of the fluid. The gravitational force per unit volume is given by:

$$\mathbf{F} = \rho \mathbf{g} \tag{3.3.7}$$

3.3.2.1.2 Electromagnetic Forces

The electromagnetic forces are composed of the electrostatic forces that depend on the net charge density and the Lorentz force that is determined by the interaction between the moving charged particles and the magnetic field. The electric force per unit volume is given by:

$$\mathbf{F} = \rho_q \mathbf{E} \tag{3.3.8}$$

The Lorentz force on the other hand is given by:

$$\mathbf{F} = \mathbf{J} \times \mathbf{B} \tag{3.3.9}$$

Here $\mathbf{J}$ is the current density given by:

$$\mathbf{J} = \sum_{\alpha} n_{\alpha} q_{\alpha} \mathbf{V}_{\alpha} \tag{3.3.10}$$

The sum is taken over all species of charged particles. In the present case two types of particles (electrons and singly charged positive ions) are considered. Assuming that the fluid is partially ionized, there are no neutral fluid particles.

A quasi–neutral the fluid is considered. This implies that the net charge density is negligibly small and hence electric force can be neglected.

3.3.2.2 Surface Forces

This forces act normally across the surface of a fluid element. Consider a fluid element of volume $d\mathscr{V}$. The fluid element is enclosed by surfaces. The fluid beyond this element exerts a force backwards onto the element hence compressing it. Considering a surface element $d\mathbf{S}$ we have the total force acting on the element given by:

$$\mathbf{f} = -\int_{S} \mathbf{P} \cdot d\mathbf{S} \tag{3.3.11}$$

Employing Gauss' theorem we have:

$$\mathbf{f} = -\int_{V} \nabla . \mathbf{P} d\mathscr{V} \tag{3.3.12}$$

In the limit $\mathscr{V} \to 0$ we have the force per unit volume given by:

$$\mathbf{F} = -\nabla \cdot \mathbf{P} \tag{3.3.13}$$

$\mathbf{P}$ in equation (3.3.13) is the stress tensor and can be decomposed as:

$$\mathbf{P} = p\mathbf{I} - \mathbf{\Pi} \tag{3.3.14}$$

Following Schnack (2009), the viscous stress tensor, $\mathbf{\Pi}$, is given by:

$$\mathbf{\Pi} = \mu\left(\nabla\mathbf{V} + \nabla\mathbf{V}^T - \frac{2}{3}\mathbf{I}\nabla\cdot\mathbf{V} \right) \tag{3.3.15}$$

This implies that the viscous force, $\nabla\cdot\mathbf{\Pi}$, becomes:

$$\mathbf{F}_\mu = \mu\left(\nabla^2\mathbf{V} - \frac{2}{3}\nabla\left(\nabla\cdot\mathbf{V}\right) \right) \tag{3.3.16}$$

In light of equation (3.3.5), the second term in the parenthesis of equation (3.3.16) vanishes. Now equation (3.3.16) becomes:

$$\mathbf{F}_\mu = \mu\nabla^2\mathbf{V} \tag{3.3.17}$$

3.3.2.3 Complete Equation of Motion

Factoring the body forces and the surface forces into equation (3.3.6) and using the total time derivative definition, $\frac{d}{dt}(\zeta) = \left(\frac{\partial}{\partial t} + \mathbf{V}\cdot\nabla \right)(\zeta)$, we have:

$$\rho\left(\frac{\partial\mathbf{V}}{\partial t} + \mathbf{V}\cdot\nabla\mathbf{V} \right) = \rho\mathbf{g} + \rho_q\mathbf{E} + \mathbf{J}\times\mathbf{B} - \nabla p + \mu\nabla^2\mathbf{V} \tag{3.3.18}$$

Equation (3.3.18) can be reduced further by the condition that the electrostatic force, $\rho_q\mathbf{E}$, is negligibly small when compared to the Lorentz force, $\mathbf{J}\times\mathbf{B}$. This is so because at all feasible lengths of MHD the net electric field is negligible. Therefore, upon neglecting $\rho_q\mathbf{E}$ from equation (3.3.18) the equation of motion becomes:

$$\rho\left(\frac{\partial \mathbf{V}}{\partial t}+\mathbf{V}\cdot\nabla\mathbf{V}\right)=\rho\mathbf{g}+\mathbf{J}\times\mathbf{B}-\nabla p+\mu\nabla^2\mathbf{V} \tag{3.3.19}$$

Following Greenspan (1963) the Coriolis force ($-2\boldsymbol{\Omega}\times\mathbf{V}$) due to rotation is introduced to equation (3.3.19) as follows:

$$\rho\left(\frac{\partial \mathbf{V}}{\partial t}+\mathbf{V}\cdot\nabla\mathbf{V}+2\boldsymbol{\Omega}\times\mathbf{V}\right)=\rho\mathbf{g}+\mathbf{J}\times\mathbf{B}-\nabla p+\mu\nabla^2\mathbf{V} \tag{3.3.20}$$

Equation (3.3.20) is the complete equation of motion of the MHD flow problem.

3.3.3 Energy Equation

The energy equation is as a result of the first law of thermodynamics. This asserts that energy can neither be created nor destroyed but transformed from one form to another. This is obtained by starting with the well known conduction equation then adding the viscous dissipation and the Joule's heating. The conduction equation is given by:

$$\rho C_p\left(\frac{\partial T}{\partial t}+\mathbf{V}\cdot\nabla T\right)=k\nabla^2 T \tag{3.3.21}$$

Adding the viscous dissipation, $\boldsymbol{\Pi}:\nabla\mathbf{V}$, and Joule's heating, $\frac{J^2}{\sigma}$, to equation (3.3.21) one obtains:

$$\rho C_p\left(\frac{\partial T}{\partial t}+\mathbf{V}\cdot\nabla T\right)=k\nabla^2 T+\boldsymbol{\Pi}:\nabla\mathbf{V}+\frac{J^2}{\sigma} \tag{3.3.22}$$

3.3.4 Mass Transfer Equation

The mass transfer equation relies on the concentration of a species in a mixture. It satisfies the principle of mass conservation but for each of the species in the fluid.

With D being the diffusion coefficient, we have the concentration equation given by:

$$\frac{dC}{dt} = D\nabla^2 C \tag{3.3.23}$$

Performing the total time derivative on the L.H.S of (3.3.23) yields:

$$\frac{\partial C}{\partial t} + \mathbf{V}\cdot\nabla C = D\nabla^2 C \tag{3.3.24}$$

3.4 Component Form of the General Governing Equations

Equations (3.3.5), (3.3.20), (3.3.22) and (3.3.24) comprise the equations governing the MHD flow problem. The four equations are summarized as follows:

$$\begin{aligned}
&\nabla\cdot\mathbf{V} = 0 \\
&\rho\left(\frac{\partial \mathbf{V}}{\partial t} + \mathbf{V}\cdot\nabla\mathbf{V} + 2\boldsymbol{\Omega}\times\mathbf{V}\right) = \rho\mathbf{g} + \mathbf{J}\times\mathbf{B} - \nabla p + \mu\nabla^2\mathbf{V} \\
&\rho C_p\left(\frac{\partial T}{\partial t} + \mathbf{V}\cdot\nabla T\right) = k\nabla^2 T + \boldsymbol{\Pi} : \nabla\mathbf{V} + \frac{J^2}{\sigma} \\
&\frac{\partial C}{\partial t} + \mathbf{V}\cdot\nabla C = D\nabla^2 C
\end{aligned} \tag{3.4.1}$$

We next write equations (3.4.1) in their respective component form. Starting with $\nabla\cdot\mathbf{V} = 0$ and defining $\mathbf{V} = u\hat{i} + v\hat{j} + w\hat{k}$, we write:

$$\frac{\partial u}{\partial x} + \frac{\partial v}{\partial y} + \frac{\partial w}{\partial z} = 0 \tag{3.4.2}$$

Since there is no velocity component in the $y - direction$ and that the plate is infinite, equation (3.4.2) reduces to:

$$\frac{\partial u}{\partial x} = \frac{\partial w}{\partial z} = 0 \tag{3.4.3}$$

We proceed to obtain the component form of the equation of motion using Boussinesq's approximation that asserts the following:

(i) All the fluid properties except for the density, ρ, are treated as constants.

(ii) The variation in density is negligible except when it directly causes buoyancy forces.

(iii) The density varies linearly with temperature and the deviation from a reference value, ρ_0, is small.

These together with the fact that the pressure gradient in the $x-$ and z directions is vanishingly small result in the component form the equation of motion in $3-D$ breaking into two parts given by:

$$\begin{aligned}\rho\left(\frac{\partial u}{\partial t}+u\frac{\partial u}{\partial x}+v\frac{\partial u}{\partial y}+w\frac{\partial u}{\partial z}+2\Omega w\right) &= -B_0 J_z+\mu\left(\frac{\partial^2 u}{\partial x^2}+\frac{\partial^2 u}{\partial y^2}+\frac{\partial^2 u}{\partial z^2}\right)\\ \rho\left(\frac{\partial w}{\partial t}+u\frac{\partial w}{\partial x}+v\frac{\partial w}{\partial y}+w\frac{\partial w}{\partial z}-2\Omega u\right) &= B_0 J_x-g\rho-\frac{\partial p}{\partial y}\\ &\quad+\mu\left(\frac{\partial^2 w}{\partial x^2}+\frac{\partial^2 w}{\partial y^2}+\frac{\partial^2 w}{\partial z^2}\right)\end{aligned} \tag{3.4.4}$$

The vertical pressure gradient is related to the free stream density as (Archimedes principle):

$$\frac{\partial p}{\partial z}=-\rho_\infty g \tag{3.4.5}$$

Substitution of relations (3.4.5) into relations (3.4.4) yields:

$$\rho\left(\frac{\partial u}{\partial t}+u\frac{\partial u}{\partial x}+v\frac{\partial u}{\partial y}+w\frac{\partial u}{\partial z}+2\Omega w\right)=-B_0J_z+\mu\left(\frac{\partial^2 u}{\partial x^2}+\frac{\partial^2 u}{\partial y^2}+\frac{\partial^2 u}{\partial z^2}\right)$$

$$\rho\left(\frac{\partial w}{\partial t}+u\frac{\partial w}{\partial x}+v\frac{\partial w}{\partial y}+w\frac{\partial w}{\partial z}-2\Omega u\right)=B_0J_x+g\left[\rho_\infty-\rho\right]+\mu\left(\frac{\partial^2 w}{\partial x^2}+\frac{\partial^2 w}{\partial y^2}+\frac{\partial^2 w}{\partial z^2}\right) \tag{3.4.6}$$

The density difference is a consequence of buoyancy and is therefore expressed in terms of the volume coefficient of expansion, β, and the concentration coefficient of expansion, β_C. Following Incropera and Dewitt (1985) we have the relations:

$$\begin{aligned}\beta&=\frac{\alpha\left(\rho_\infty-\rho\right)}{\rho\left(T-T_\infty\right)}\Rightarrow\beta\rho\left(T-T_\infty\right)=\alpha\left(\rho_\infty-\rho\right)\\ \beta_C&=\frac{\left(1-\alpha\right)\left(\rho_\infty-\rho\right)}{\rho\left(C-C_\infty\right)}\Rightarrow\beta_C\rho\left(C-C_\infty\right)=\left(1-\alpha\right)\left(\rho_\infty-\rho\right)\end{aligned} \tag{3.4.7}$$

In relations (3.4.7) α is the thermal contribution factor while $1-\alpha$ is the concentration contribution to buoyancy. Summing up the relations (3.4.7) we obtain the difference in densities as:

$$\rho_\infty-\rho=\rho\left[\beta\left(T-T_\infty\right)+\beta_C\left(C-C_\infty\right)\right] \tag{3.4.8}$$

Substituting equation (3.4.8) into relations (3.4.6) one obtains:

$$\begin{aligned}\rho\left(\frac{\partial u}{\partial t}+u\frac{\partial u}{\partial x}+v\frac{\partial u}{\partial y}+w\frac{\partial u}{\partial z}+2\Omega w\right)&=-B_0J_z+\mu\left(\frac{\partial^2 u}{\partial x^2}+\frac{\partial^2 u}{\partial y^2}+\frac{\partial^2 u}{\partial z^2}\right)\\ \rho\left(\frac{\partial w}{\partial t}+u\frac{\partial w}{\partial x}+v\frac{\partial w}{\partial y}+w\frac{\partial w}{\partial z}-2\Omega u\right)&=B_0J_x\\ &\quad+g\rho\left[\beta\left(T-T_\infty\right)+\beta_C\left(C-C_\infty\right)\right]\\ &\quad+\mu\left(\frac{\partial^2 w}{\partial x^2}+\frac{\partial^2 w}{\partial y^2}+\frac{\partial^2 w}{\partial z^2}\right)\end{aligned} \tag{3.4.9}$$

Due to the geometry of the problem all derivatives w.r.t x and z vanish. There is no y – component of the velocity. Equations (3.4.9) then reduce to:

$$\frac{\partial u}{\partial t}+2\Omega w=\frac{-B_0 J_z}{\rho}+\upsilon\frac{\partial^2 u}{\partial y^2}$$
$$\frac{\partial w}{\partial t}-2\Omega u=\frac{B_0 J_x}{\rho}+g\left[\beta\left(T-T_\infty\right)+\beta_C\left(C-C_\infty\right)\right]+\upsilon\frac{\partial^2 w}{\partial y^2} \qquad (3.4.10)$$

Following Schlchiting (1979), the viscous dissipation term $\mathbf{\Pi}:\nabla\mathbf{V}$ in the energy equation given by:

$$\mathbf{\Pi}:\nabla\mathbf{V}=\mu\left\{2\left[\left(\frac{\partial u}{\partial x}\right)^2+\left(\frac{\partial v}{\partial y}\right)^2+\left(\frac{\partial w}{\partial z}\right)^2\right]+\left(\frac{\partial u}{\partial y}+\frac{\partial v}{\partial x}\right)^2+\left(\frac{\partial v}{\partial z}+\frac{\partial w}{\partial y}\right)^2+\left(\frac{\partial w}{\partial x}+\frac{\partial u}{\partial z}\right)^2\right\}$$
$$=\mu\left[\left(\frac{\partial u}{\partial y}\right)^2+\left(\frac{\partial w}{\partial y}\right)^2\right] \qquad (3.4.11)$$

Substituting (3.4.11) into the energy equation and using the fact that all derivatives w.r.t x and z vanish, the energy equation in component form becomes:

$$\rho C_p\frac{\partial T}{\partial t}=k\frac{\partial^2 T}{\partial y^2}+\mu\left[\left(\frac{\partial u}{\partial y}\right)^2+\left(\frac{\partial w}{\partial y}\right)^2\right]+\frac{1}{\sigma}\left(J_x{}^2+J_z{}^2\right) \qquad (3.4.12)$$

Similarly the concentration equation becomes:

$$\frac{\partial C}{\partial t}=D\frac{\partial^2 C}{\partial y^2} \qquad (3.4.13)$$

Equations (3.4.3), (3.4.10), (3.4.12) and (3.4.13) give the general governing equations in component form.

3.5 Turbulence Effects

Above some critical Reynold's number, Re_{cr}, all fluid flows become turbulent. The flow variables e.g. velocity, pressure and temperature undergo chaotic

fluctuations. Several approaches have been suggested to deal with the turbulence phenomenon (Del Sordo *et al*, 2013). Among them is the Reynold's Averaged Navier Stokes (RANS) which we shall be using. In this approach, the flow variable is decomposed into an average (taken over an appropriate time interval) and a perturbation to take care of the fluctuations. Taking ζ as the flow variable, one has:

$$\zeta = \bar{\zeta} + \zeta' \tag{3.5.1}$$

Where $\bar{\zeta}$ is the average value and ζ' is the perturbation due to the fluctuations. After the perturbative treatment of every flow variable, we next average the entire equation over the time interval, Δt . Some of the guidelines in Reynold's Averaging are:

$$\begin{array}{lll} \phi = \bar{\phi} + \phi', & \varsigma = \bar{\varsigma} + \varsigma' & \\ \bar{\bar{\phi}} = \bar{\phi}, & \overline{\phi + \varsigma} = \bar{\phi} + \bar{\varsigma}, & \overline{\mathscr{C}\phi} = \mathscr{C}\bar{\phi} \\ \overline{\bar{\phi}\varsigma} = \bar{\phi}\bar{\varsigma}, & \overline{\phi\varsigma} \neq \bar{\phi}\bar{\varsigma}, & \overline{\frac{\partial \phi}{\partial \vartheta}} = \frac{\partial \bar{\phi}}{\partial \vartheta} \end{array} \tag{3.5.2}$$

In equation (3.5.2) $\mathscr{C}$ is an arbitrary constant while ϑ is an independent variable.

3.5.1 The Continuity Equation with Turbulence

Taking the turbulence perturbation into equation (3.4.2) we write:

$$\frac{\partial}{\partial x}\left(\bar{u} + u'\right) + \frac{\partial}{\partial y}\left(\bar{v} + v'\right) + \frac{\partial}{\partial z}\left(\bar{w} + w'\right) = 0$$

$$\text{Upon averaging:} \tag{3.5.3}$$

$$\frac{\partial \bar{u}}{\partial x} + \frac{\partial \bar{v}}{\partial y} + \frac{\partial \bar{w}}{\partial z} = 0$$

Since there is no varying $y-$component of velocity and, because the plate is infinite, derivatives along x and z are identically zero, we have:

$$\frac{\partial \overline{u}}{\partial x} = \frac{\partial \overline{w}}{\partial z} = 0 \tag{3.5.4}$$

3.5.2 The Equation of Motion with Turbulence

Allowing the turbulence perturbation into equation (3.4.9), we have:

$$\begin{aligned}
&\rho\left(\frac{\partial}{\partial t}(\overline{u}+u')+(\overline{u}+u')\frac{\partial}{\partial x}(\overline{u}+u')+(\overline{v}+v')\frac{\partial}{\partial y}(\overline{u}+u')\right.\\
&\qquad\left.+(\overline{w}+w')\frac{\partial}{\partial z}(\overline{u}+u')+2\Omega(\overline{w}+w')\right)\\
&\qquad=-B_0J_z+\mu\left(\frac{\partial^2}{\partial x^2}(\overline{u}+u')+\frac{\partial^2}{\partial y^2}(\overline{u}+u')+\frac{\partial^2}{\partial z^2}(\overline{u}+u')\right)\\
&\rho\left(\frac{\partial}{\partial t}(\overline{w}+w')+(\overline{u}+u')\frac{\partial}{\partial x}(\overline{w}+w')+(\overline{v}+v')\frac{\partial}{\partial y}(\overline{w}+w')\right.\\
&\qquad\left.+(\overline{w}+w')\frac{\partial}{\partial z}(\overline{w}+w')-2\Omega(\overline{u}+u')\right)\\
&\qquad=B_0J_x+g\rho\left[\beta(T-T_\infty)+\beta_C(C-C_\infty)\right]\\
&\qquad\qquad+\mu\left(\frac{\partial^2}{\partial x^2}(\overline{w}+w')+\frac{\partial^2}{\partial y^2}(\overline{w}+w')+\frac{\partial^2}{\partial z^2}(\overline{w}+w')\right)
\end{aligned} \tag{3.5.5}$$

In equation (3.5.5) the temperature and concentration fluctuations have been neglected. Noticing that derivatives along x and z are identically zero, we average the pair of equations to get:

$$\begin{aligned}
&\frac{\partial \overline{u}}{\partial t}+\overline{v}\frac{\partial \overline{u}}{\partial y}+2\Omega\overline{w}=\frac{-B_0J_z}{\rho}+\upsilon\frac{\partial^2\overline{u}}{\partial y^2}-\frac{\partial\overline{vu}}{\partial y}\\
&\frac{\partial \overline{w}}{\partial t}+\overline{v}\frac{\partial \overline{w}}{\partial y}-2\Omega\overline{u}=\frac{B_0J_x}{\rho}+g\left[\beta(T-T_\infty)+\beta_C(C-C_\infty)\right]+\upsilon\frac{\partial^2\overline{w}}{\partial y^2}-\frac{\partial\overline{vw}}{\partial y}
\end{aligned} \tag{3.5.6}$$

Although there is no $y-$component of velocity, we assume a small drag velocity, v_o, due to injection or suction. In equations (3.5.6) the last terms on the R.H.S involve mixtures of velocities. This can be simplified by employing Prandtl mixing length hypothesis which asserts (McComb, 1990):

$$\begin{aligned}\rho\overline{vw} &= -\rho l^2\left(\frac{\partial\overline{v}}{\partial z}\right)\\ &= -\rho\kappa^2 z^2\left(\frac{\partial\overline{v}}{\partial z}\right)\\ \Rightarrow \overline{vw} &= -\kappa^2 z^2\left(\frac{\partial\overline{v}}{\partial z}\right)\end{aligned} \tag{3.5.7}$$

Where $l=\kappa z$ and κ is the von Karman constant in relation (3.5.7).

In a similar way we have:

$$\begin{aligned}\overline{vu} &= -\kappa^2 y^2\left(\frac{\partial\overline{u}}{\partial y}\right)\\ \overline{vw} &= -\kappa^2 y^2\left(\frac{\partial\overline{w}}{\partial y}\right)\end{aligned} \tag{3.5.8}$$

Substituting relations (3.5.8) into equations (3.5.6) yields:

$$\begin{aligned}\frac{\partial\overline{u}}{\partial t}+\overline{v}\frac{\partial\overline{u}}{\partial y}+2\Omega\overline{w} &= \frac{-B_0 J_z}{\rho}+\upsilon\frac{\partial^2\overline{u}}{\partial y^2}+2\kappa^2\left[y\left(\frac{\partial\overline{u}}{\partial y}\right)^2+y^2\left(\frac{\partial\overline{u}}{\partial y}\right)\left(\frac{\partial^2\overline{u}}{\partial y^2}\right)\right]\\ \frac{\partial\overline{w}}{\partial t}+\overline{v}\frac{\partial\overline{w}}{\partial y}-2\Omega\overline{u} &= \frac{B_0 J_x}{\rho}+g\left[\beta\left(T-T_\infty\right)+\beta_C\left(C-C_\infty\right)\right]+\upsilon\frac{\partial^2\overline{w}}{\partial y^2}\\ &\quad +2\kappa^2\left[y\left(\frac{\partial\overline{w}}{\partial y}\right)^2+y^2\left(\frac{\partial\overline{w}}{\partial y}\right)\left(\frac{\partial^2\overline{w}}{\partial y^2}\right)\right]\end{aligned} \tag{3.5.9}$$

3.5.3 The Energy Equation with Turbulence

Applying the same procedure as we did for continuity and momentum equations to (3.4.12) and including the term, $\overline{v}\frac{\partial T}{\partial y}$, due the total time derivative on the L.H.S we obtain:

$$\rho C_p\left(\frac{\partial T}{\partial t}+\overline{v}\frac{\partial T}{\partial y}\right)=k\frac{\partial^2 T}{\partial y^2}+\mu\left[\left(\frac{\partial\overline{u}}{\partial y}\right)^2+\left(\frac{\partial\overline{w}}{\partial y}\right)^2\right]+\frac{1}{\sigma}\left(J_x{}^2+J_z{}^2\right) \tag{3.5.10}$$

In the above equation we set $T = \bar{T}$ to imply that the temperature fluctuations are negligible.

3.5.4 The Concentration Equation with Turbulence

The concentration, C, just like the temperature, will be negligibly perturbed. Applying the perturbation procedure to equation (3.4.13) and including the term, $\bar{v}\frac{\partial C}{\partial y}$, due the total time derivative on the L.H.S we obtain:

$$\frac{\partial C}{\partial t} + \bar{v}\frac{\partial C}{\partial y} = D\frac{\partial^2 C}{\partial y^2} \tag{3.5.11}$$

Again the fluctuation of the concentration is taken to be negligibly small in equation (3.5.11).

3.6 Hall Current Effect

3.6.1 General Ohm's Law

The generalized Ohm's law that includes Hall currents, ion slip currents and electron pressure gradient is given as:

$$\begin{aligned}\mathbf{J} + \frac{\omega_e \tau_e}{|\mathbf{B}|}\left(1 - \frac{\omega_i \tau_i}{|\mathbf{B}|}\right)(\mathbf{J}\times\mathbf{B}) &= \sigma\frac{\left(\mathbf{E} + \mathbf{V}\times\mathbf{B} - \frac{1}{ne}\nabla p_e\right)}{\sqrt{1 - \frac{V^2}{c^2}}} \\ &= \sigma\left(\mathbf{E} + \mathbf{V}\times\mathbf{B} - \frac{1}{ne}\nabla p_e\right)\left(1 - \frac{1}{2}\frac{V^2}{c^2} + \cdots\right)\end{aligned} \tag{3.6.1}$$

In MHD the assumption is that the fluid velocity is negligibly small compared to the speed of light i.e. $V \ll c \;\Rightarrow\; \frac{1}{2}\frac{V^2}{c^2} \ll 1$. Further, considering a short circuit problem, $\mathbf{E} = 0$. For partially ionized fluids, the pressure gradient is negligible.

Last, the ion slip currents are too small since the mass of an ion is heavy and cannot lead to high cyclotron velocities i.e. $\frac{\omega_i \tau_i}{|\mathbf{B}|} \ll 1$. With these assumptions, equation (3.6.1) becomes:

$$\mathbf{J} + \frac{\omega_e \tau_e}{|\mathbf{B}|}(\mathbf{J} \times \mathbf{B}) = \sigma \mathbf{V} \times \mathbf{B} \tag{3.6.2}$$

By the definition $\mathbf{B} = \mu_e \mathbf{H}$ and the fact that we have a strong applied magnetic field, $|\mathbf{B}| = B_0 = \mu_e H_0$, equation (3.6.2) can be written as:

$$\mathbf{J} + \frac{\omega_e \tau_e}{H_0}(\mathbf{J} \times \mathbf{H}) = \sigma \mu_e \mathbf{V} \times \mathbf{H} \tag{3.6.3}$$

Resolution of (3.6.3) into its component form yields the pair of equations:

$$\begin{aligned} J_x - \omega_e \tau_e J_z &= -\sigma \mu_e H_0 w \\ \omega_e \tau_e J_x + J_z &= \sigma \mu_e H_0 u \end{aligned} \tag{3.6.4}$$

There is no current component in the $y-$direction since the applied magnetic field is along the same direction. Solving the system (3.6.4) of simultaneous equations in J_x and J_z and using the definition of the Hall parameter, $m = \omega_e \tau_e$, yields:

$$\begin{aligned} J_x &= \frac{\sigma \mu_e H_0}{1+m^2}(mu - w) \\ J_z &= \frac{\sigma \mu_e H_0}{1+m^2}(mw + u) \end{aligned} \tag{3.6.5}$$

Squaring both sides of (3.6.5) one obtains:

$$\begin{aligned} J_x{}^2 &= \sigma^2 \mu_e{}^2 H_0{}^2 \left(\frac{mu - w}{1+m^2}\right)^2 \\ J_z{}^2 &= \sigma^2 \mu_e{}^2 H_0{}^2 \left(\frac{mw + u}{1+m^2}\right)^2 \end{aligned} \tag{3.6.6}$$

3.6.2 Momentum and Energy Equations with Hall Currents

Substituting equations (3.6.5) into the equation of motion (3.5.9) we obtain:

$$\begin{aligned}\frac{\partial \bar{u}}{\partial t}+\bar{v}\frac{\partial \bar{u}}{\partial y}+2\Omega\bar{w}&=\frac{-\sigma{\mu_e}^2{H_0}^2}{\rho\left(1+m^2\right)}\left(m\bar{w}+\bar{u}\right)+\upsilon\frac{\partial^2\bar{u}}{\partial y^2}\\&\quad+2\kappa^2\left[y\left(\frac{\partial \bar{u}}{\partial y}\right)^2+y^2\left(\frac{\partial \bar{u}}{\partial y}\right)\left(\frac{\partial^2\bar{u}}{\partial y^2}\right)\right]\\\frac{\partial \bar{w}}{\partial t}+\bar{v}\frac{\partial \bar{w}}{\partial y}-2\Omega\bar{u}&=\frac{\sigma{\mu_e}^2{H_0}^2}{\rho\left(1+m^2\right)}\left(m\bar{u}-\bar{w}\right)+g\left[\beta\left(T-T_\infty\right)+\beta_C\left(C-C_\infty\right)\right]\\&\quad+\upsilon\frac{\partial^2\bar{w}}{\partial y^2}+2\kappa^2\left[y\left(\frac{\partial \bar{w}}{\partial y}\right)^2+y^2\left(\frac{\partial \bar{w}}{\partial y}\right)\left(\frac{\partial^2\bar{w}}{\partial y^2}\right)\right]\end{aligned}\tag{3.6.7}$$

Substituting equations (3.6.6) into the energy equation (3.5.10) one obtains:

$$\begin{aligned}\rho C_p\left(\frac{\partial T}{\partial t}+\bar{v}\frac{\partial T}{\partial y}\right)&=k\frac{\partial^2 T}{\partial y^2}+\mu\left[\left(\frac{\partial \bar{u}}{\partial y}\right)^2+\left(\frac{\partial \bar{w}}{\partial y}\right)^2\right]\\&\quad+\frac{\sigma{\mu_e}^2{H_0}^2}{\left(1+m^2\right)^2}\left[\left(m\bar{u}-\bar{w}\right)^2+\left(m\bar{w}+\bar{u}\right)^2\right]\end{aligned}\tag{3.6.8}$$

3.7 Non–Dimensionalisation

3.7.1 Importance of Non–Dimensionalisation

Non–dimensionalisation has both the ability to reduce a complicated physical problem into a more feasible one for solutions and also enables the scientists work with models without limiting themselves to specific measurements and units (Schaschke, 1998). Theoretical solutions obtained in non–dimensional form are more flexible and free of units. In the present MHD problem, the dimensional form of the governing equations shall be given before embarking on the non–dimensionalisation process.

3.7.2 Governing Equations in Dimensional Form

A flow variable, ζ, is denoted as ζ^* in dimensional form. From equations (3.6.7), (3.6.8) and (3.5.11) we have the dimensional form of momentum, energy and concentration equations respectively as:

$$\begin{aligned}\frac{\partial u^*}{\partial t^*}+v_0^*\frac{\partial u^*}{\partial y^*}+2\Omega w^* &= \frac{-\sigma {\mu_e}^2 {H_0}^2}{\rho\left(1+m^2\right)}\left(mw^*+u^*\right)+\upsilon\frac{\partial^2 u^*}{\partial y^{*2}}\\ &\quad +2\kappa^2\left[y^*\left(\frac{\partial u^*}{\partial y^*}\right)^2+y^{*2}\left(\frac{\partial u^*}{\partial y^*}\right)\left(\frac{\partial^2 u^*}{\partial y^{*2}}\right)\right]\\ \frac{\partial w^*}{\partial t^*}+v_0^*\frac{\partial w^*}{\partial y^*}-2\Omega u^* &= \frac{\sigma {\mu_e}^2 {H_0}^2}{\rho\left(1+m^2\right)}\left(mu^*-w^*\right)\\ &\quad +g\left[\beta\left(T^*-T_\infty^*\right)+\beta_C\left(C^*-C_\infty^*\right)\right]+\upsilon\frac{\partial^2 w^*}{\partial y^{*2}}\\ &\quad +2\kappa^2\left[y^*\left(\frac{\partial w^*}{\partial y^*}\right)^2+y^{*2}\left(\frac{\partial w^*}{\partial y^*}\right)\left(\frac{\partial^2 w^*}{\partial y^{*2}}\right)\right]\end{aligned} \tag{3.7.1}$$

$$\begin{aligned}\rho C_p\left(\frac{\partial T^*}{\partial t^*}+v_0^*\frac{\partial T^*}{\partial y^*}\right) &= k\frac{\partial^2 T^*}{\partial y^{*2}}+\mu\left[\left(\frac{\partial u^*}{\partial y^*}\right)^2+\left(\frac{\partial w^*}{\partial y^*}\right)^2\right]\\ &\quad +\frac{\sigma {\mu_e}^2 {H_0}^2}{\left(1+m^2\right)^2}\left[\left(mu^*-w^*\right)^2+\left(mw^*+u^*\right)^2\right]\end{aligned} \tag{3.7.2}$$

$$\frac{\partial C^*}{\partial t^*}+v_0^*\frac{\partial C^*}{\partial y^*}=D\frac{\partial^2 C^*}{\partial y^{*2}} \tag{3.7.3}$$

In equations (3.7.1), (3.7.2) and (3.7.3) we dropped the bars above the velocities and replaced $\bar{v}^*$ with v_0^*. The initial and boundary conditions given by:

$$\begin{array}{llll} t^*<0: u^*=0, & w^*=0, & T^*=T_\infty^*, & C^*=C_\infty^* \,\|\, \text{Everywhere}\\ t^*\geq 0: u^*=U_0, & w^*=W_0, & T^*=T_w^*, & C^*=C_w^* \,\|\, \text{At } y=0\\ \quad : u^*\to 0, & w^*\to 0, & T^*\to T_\infty^*, & C^*\to C_\infty^* \,\|\, As\ y\to\infty \end{array} \tag{3.7.4}$$

3.7.3 Non–Dimensional Variables

To allow for independence of units and scales, dimensionless groups are employed. The characteristic values for velocity, pressure, length, time and magnetic field are denoted by the letters U, P, L, t and H respectively. We define the following non–dimensional variables for the present MHD problem:

$$t=\frac{t^*U^2}{\upsilon},\qquad y=\frac{y^*U}{\upsilon},\qquad u=\frac{u^*}{U},\qquad v_0=\frac{v_0^*}{U},\qquad w=\frac{w^*}{U},$$
$$\theta=\frac{T^*-T_\infty^*}{T_w^*-T_\infty^*},\quad C=\frac{C^*-C_\infty^*}{C_w^*-C_\infty^*} \tag{3.7.5}$$

With the dimensionless variables above, we evaluate:

$$\frac{\partial u^*}{\partial t^*}=\frac{\partial u^*}{\partial u}\frac{\partial u}{\partial t}\frac{\partial t}{\partial t^*}=\frac{U^3}{\upsilon}\frac{\partial u}{\partial t},\ \frac{\partial u^*}{\partial y^*}=\frac{\partial u^*}{\partial u}\frac{\partial u}{\partial y}\frac{\partial y}{\partial y^*}=\frac{U^2}{\upsilon}\frac{\partial u}{\partial y},\ v_0^*\frac{\partial u^*}{\partial y^*}=\frac{U^3}{\upsilon}v_0\frac{\partial u}{\partial y}$$
$$\upsilon\frac{\partial^2 u^*}{\partial y^{*2}}=\upsilon\frac{\partial}{\partial y}\left(\frac{\partial u^*}{\partial y^*}\right)\frac{\partial y}{\partial y^*}=\upsilon\frac{\partial}{\partial y}\left(\frac{U^2}{\upsilon}\frac{\partial u}{\partial y}\right)\frac{U}{\upsilon}=\frac{U^3}{\upsilon}\frac{\partial^2 u}{\partial y^2},\quad 2\Omega w^*=2U\Omega w,$$
$$y^*\left(\frac{\partial u^*}{\partial y^*}\right)^2=\frac{\upsilon}{U}y\left(\frac{U^2}{\upsilon}\frac{\partial u}{\partial y}\right)^2=\frac{U^3}{\upsilon}y\left(\frac{\partial u}{\partial y}\right)^2,\quad mw^*+u^*=U\left(mw+u\right), \tag{3.7.6}$$
$$y^{*2}\left(\frac{\partial u^*}{\partial y^*}\right)\left(\frac{\partial^2 u^*}{\partial y^{*2}}\right)=\left(\frac{\upsilon}{U}y\right)^2\left(\frac{U^2}{\upsilon}\frac{\partial u}{\partial y}\right)\left(\frac{U^3}{\upsilon^2}\frac{\partial^2 u}{\partial y^2}\right)=\frac{U^3}{\upsilon}y^2\left(\frac{\partial u}{\partial y}\right)\left(\frac{\partial^2 u}{\partial y^2}\right)$$

Similarly we evaluate:

$$\frac{\partial w^*}{\partial t^*}=\frac{U^3}{\upsilon}\frac{\partial w}{\partial t},\ v_0^*\frac{\partial w^*}{\partial y^*}=\frac{U^3}{\upsilon}v_0\frac{\partial w}{\partial y},\ 2\Omega u^*=2U\Omega u, mu^*-w^*=U\left(mu-w\right),$$
$$\upsilon\frac{\partial^2 w^*}{\partial y^{*2}}=\frac{U^3}{\upsilon}\frac{\partial^2 w}{\partial y^2},\ y^*\left(\frac{\partial w^*}{\partial y^*}\right)^2=\frac{U^3}{\upsilon}y\left(\frac{\partial w}{\partial y}\right)^2,\beta\left(T^*-T_\infty^*\right)=\beta\theta\left(T_w^*-T_\infty^*\right), \tag{3.7.7}$$
$$y^{*2}\left(\frac{\partial w^*}{\partial y^*}\right)\left(\frac{\partial^2 w^*}{\partial y^{*2}}\right)=\frac{U^3}{\upsilon}y^2\left(\frac{\partial w}{\partial y}\right)\left(\frac{\partial^2 w}{\partial y^2}\right),\beta_C\left(C^*-C_\infty^*\right)=\beta_C C\left(C_w^*-C_\infty^*\right)$$

For the energy equation we evaluate the following:

$$\frac{\partial T^*}{\partial t^*} = \frac{\partial T^*}{\partial \theta}\frac{\partial \theta}{\partial t}\frac{\partial t}{\partial t^*} = \frac{U^2}{\upsilon}\left(T_w^* - T_\infty^*\right)\frac{\partial \theta}{\partial t},$$
$$v_0^*\frac{\partial T^*}{\partial y^*} = Uv_0\frac{\partial T^*}{\partial \theta}\frac{\partial \theta}{\partial y}\frac{\partial y}{\partial y^*} = \frac{U^2}{\upsilon}v_0\left(T_w^* - T_\infty^*\right)\frac{\partial \theta}{\partial y} \qquad (3.7.8)$$
$$k\frac{\partial^2 T^*}{\partial y^{*2}} = k\frac{\partial}{\partial y}\left(\frac{\partial T^*}{\partial y^*}\right)\frac{\partial y}{\partial y^*} = \frac{kU^2}{\upsilon^2}\left(T_w^* - T_\infty^*\right)\frac{\partial^2 \theta}{\partial t^2}$$

For the concentration equation we evaluate:

$$\frac{\partial C^*}{\partial t^*} = \frac{\partial C^*}{\partial C}\frac{\partial C}{\partial t}\frac{\partial t}{\partial t^*} = \frac{U^2}{\upsilon}\left(C_w^* - C_\infty^*\right)\frac{\partial C}{\partial t},\ v_0^*\frac{\partial C^*}{\partial y^*} = \frac{U^2}{\upsilon}\left(C_w^* - C_\infty^*\right)v_o\frac{\partial C}{\partial y}$$
$$D\frac{\partial^2 C^*}{\partial y^{*2}} = D\frac{\partial}{\partial y}\left(\frac{\partial C^*}{\partial y^*}\right)\frac{\partial y}{\partial y^*} = \frac{DU^2}{\upsilon^2}\left(C_w^* - C_\infty^*\right)\frac{\partial^2 C}{\partial y^2} \qquad (3.7.9)$$

Substituting relations (3.7.6) and (3.7.7) into equations (3.7.1) and dividing through by $\frac{U^3}{\upsilon}$ yields the momentum equations as:

$$\frac{\partial u}{\partial t} + v_0\frac{\partial u}{\partial y} + \frac{2\upsilon\Omega}{U^2}w = \frac{-\sigma{\mu_e}^2{H_0}^2\upsilon}{\rho U^2\left(1+m^2\right)}\left(mw+u\right) + \frac{\partial^2 u}{\partial y^2}$$
$$+ 2\kappa^2\left[y\left(\frac{\partial u}{\partial y}\right)^2 + y^2\left(\frac{\partial u}{\partial y}\right)\left(\frac{\partial^2 u}{\partial y^2}\right)\right]$$
$$\frac{\partial w}{\partial t} + v_0\frac{\partial w}{\partial y} - \frac{2\upsilon\Omega}{U^2}u = \frac{\sigma{\mu_e}^2{H_0}^2\upsilon}{\rho U^2\left(1+m^2\right)}\left(mu-w\right) \qquad (3.7.10)$$
$$+ \frac{g\upsilon}{U^3}\left[\beta\theta\left(T_w^* - T_\infty^*\right) + \beta_C C\left(C_w^* - C_\infty^*\right)\right] + \frac{\partial^2 w}{\partial y^2}$$
$$+ 2\kappa^2\left[y\left(\frac{\partial w}{\partial y}\right)^2 + y^2\left(\frac{\partial w}{\partial y}\right)\left(\frac{\partial^2 w}{\partial y^2}\right)\right]$$

Substituting relations (3.7.6), (3.7.7) and (3.7.8) into (3.7.2) and dividing through by $\frac{\rho C_p U^2}{\upsilon}\left(T_w^* - T_\infty^*\right)$ yields the energy equation as:

$$\frac{\partial\theta}{\partial t}+v_0\frac{\partial\theta}{\partial y}=\frac{k}{\upsilon\rho C_p}\frac{\partial^2\theta}{\partial y^2}+\frac{U^2}{C_p\left(T_w^*-T_\infty^*\right)}\left[\left(\frac{\partial u}{\partial y}\right)^2+\left(\frac{\partial w}{\partial y}\right)^2\right] + \frac{\upsilon\sigma{\mu_e}^2{H_0}^2}{\rho C_p\left(1+m^2\right)^2\left(T_w^*-T_\infty^*\right)}\left[\left(mu-w\right)^2+\left(mw+u\right)^2\right] \tag{3.7.11}$$

Substituting relations (3.7.9) into equation (3.7.3) and dividing through by $\frac{U^2}{\upsilon}\left(C_w^*-C_\infty^*\right)$ yields the concentration equation as:

$$\frac{\partial C}{\partial t}+v_0\frac{\partial C}{\partial y}=\frac{D}{\upsilon}\frac{\partial^2 C}{\partial y^2} \tag{3.7.12}$$

3.7.4 Common Non–Dimensional Numbers and Parameters in MHD

Equations (3.7.10), (3.7.11) and (3.7.12) can be simplified further by employing common non–dimensional numbers and parameters. In this section we describe a few of these numbers and parameters that will be used in the current problem.

3.7.4.1 Prandtl Number

This number describes the ratio of momentum diffusivity to heat diffusivity. A high Prandtl number indicates that heat diffuses very slowly relative to momentum while a low Prandtl number indicates that heat diffuses very fast relative to momentum. A Prandtl number of about 1 implies that heat and momentum are diffused within the material at almost the same rate. The Prandtl number is given by:

$$Pr=\frac{\mu C_p}{k} \tag{3.7.13}$$

3.7.4.2 Grashof Number

The Grashof number represents the ratio of buoyancy forces to viscous forces. It is given by:

$$Gr_L = \frac{\upsilon g \beta \left(T_w - T_\infty\right)}{U^3} \tag{3.7.14}$$

Due to relative similarities, we define the concentration variant of the Grashof number as:

$$Gr_C = \frac{\upsilon g \beta_C \left(C_w - C_\infty\right)}{U^3} \tag{3.7.15}$$

3.7.4.3 Eckert Number

The Eckert number provides a measure of the kinetic energy of the flow relative to the enthalpy difference. It is given by:

$$Ec = \frac{U^2}{C_p \left(T_w - T_\infty\right)} \tag{3.7.16}$$

3.7.4.4 Schmidt Number

The Schmidt number represents the ratio of momentum diffusivity to mass diffusivity. A high Schmidt number implies that mass transfer by diffusion is low compared to the momentum diffusion. A low Schmidt number on the other hand implies that mass transfer by diffusion is relatively high. The Schmidt number is given by:

$$Sc = \frac{\upsilon}{D} \tag{3.7.17}$$

3.7.4.5 Magnetic Parameter

This is the ratio of the magnetic force to the viscous force. The magnetic parameter is given by:

$$M^2 = \frac{\sigma \mu_e{}^2 H_o{}^2 \upsilon}{\rho U^2} \tag{3.7.18}$$

3.7.4.6 Rotational Parameter

The rotational parameter is the ratio of angular kinetic energy to translational kinetic energy and is given by:

$$Er = \frac{\Omega \upsilon}{U^2} \tag{3.7.19}$$

3.8 Final Set of Governing Equations

With the non–dimensional quantities defined in equations (3.7.13) – (3.7.19) further simplification of the equation of motion (3.7.10), the energy equation (3.7.11) and the concentration equation (3.7.12) is attained as:

$$\begin{aligned}
&\frac{\partial u}{\partial t} + v_0 \frac{\partial u}{\partial y} + 2Erw = -\frac{M^2}{1+m^2}(mw+u) + \frac{\partial^2 u}{\partial y^2} \\
&\qquad + 2\kappa^2 \left[y\left(\frac{\partial u}{\partial y}\right)^2 + y^2 \left(\frac{\partial u}{\partial y}\right)\left(\frac{\partial^2 u}{\partial y^2}\right) \right] \\
&\frac{\partial w}{\partial t} + v_0 \frac{\partial w}{\partial y} - 2Eru = \frac{M^2}{1+m^2}(mu-w) + \left[Gr_L \theta + Gr_C C\right] \\
&\qquad + \frac{\partial^2 w}{\partial y^2} + 2\kappa^2 \left[y\left(\frac{\partial w}{\partial y}\right)^2 + y^2 \left(\frac{\partial w}{\partial y}\right)\left(\frac{\partial^2 w}{\partial y^2}\right) \right]
\end{aligned} \tag{3.8.1}$$

$$\frac{\partial \theta}{\partial t} + v_0 \frac{\partial \theta}{\partial y} = \frac{1}{Pr}\frac{\partial^2 \theta}{\partial y^2} + Ec\left[\left(\frac{\partial u}{\partial y}\right)^2 + \left(\frac{\partial w}{\partial y}\right)^2\right] + \frac{EcM^2}{\left(1+m^2\right)^2}\left[\left(mu - w\right)^2 + \left(mw + u\right)^2\right] \tag{3.8.2}$$

$$\frac{\partial C}{\partial t} + v_0 \frac{\partial C}{\partial y} = \frac{1}{Sc}\frac{\partial^2 C}{\partial y^2} \tag{3.8.3}$$

Equations (3.8.1), (3.8.2) and (3.8.3) are the final governing equations of the MHD fluid flow problem described in section 1.4. The corresponding initial and boundary conditions are:

$$\begin{aligned} t < 0 &: U = 0, \quad W = 0, \quad \theta = 0, \quad C = 0 \,\|\, everywhere \\ t \geq 0 &: U = 0, \quad W = 1, \quad \theta = 1, \quad C = 1 \,\|\, at\ y = 0 \\ &: U \to 0, \quad V \to 0, \quad \theta \to 0, \quad C \to 0 \,\|\, as\ y \to \infty \end{aligned} \tag{3.8.4}$$

In the next chapter we develop a numerical scheme corresponding to the final set of governing equations in view of the boundary conditions.

CHAPTER FOUR

NUMERICAL TECHNIQUE

4.1 Overview

The final set of governing equations: (3.8.1), (3.8.2) and (3.8.3) cannot be solved analytically since they are highly coupled and nonlinear. Together with the boundary conditions (3.8.4), a numerical solution is constructed using the finite difference method (FDM). The velocity, temperature and concentration are all functions of time (t) and space (y). There is, therefore, a necessity to discretize the time and space coordinates to form a solution mesh. In this chapter we discuss the solution mesh, the finite difference method, the difference equations and the resultant computer program.

4.2 Computation Grid

To begin the discretization process, we define the computation grid or mesh. This will be a rectangular mesh with the space co-ordinate along the horizontal axis and the temporal co-ordinate along the vertical axis. The space co-ordinate is subdivided into $N-1$ intervals of equal length Δy so that there are N nodal points. On the other hand, the temporal co-ordinate is subdivided into $K-1$ intervals of equal length Δt so that there are K nodal points.

Each of the nodal points is labelled by a pair of indices, j and k. The functions u, w, θ and C are evaluated at each nodal point. Below is a schematic diagram (Figure 4. 1) of the representative mesh.

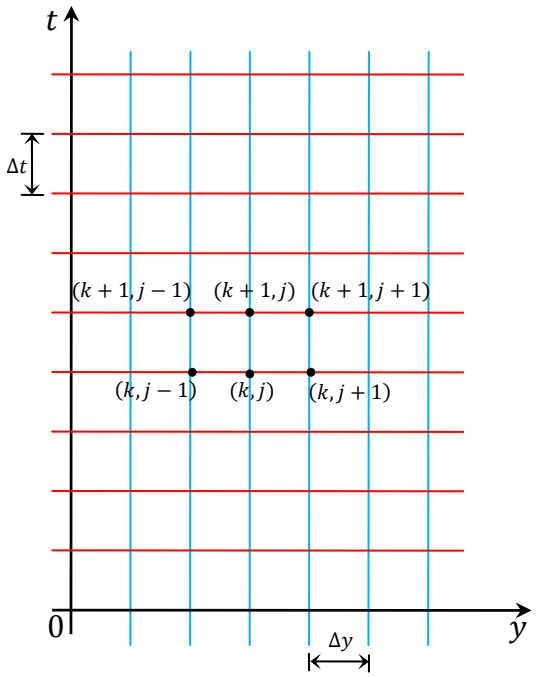

Figure 4. 1: Computation grid representation

4.3 Finite Difference Methods

4.3.1 Temporal Partial Derivative

Partial derivatives with respect to time are evaluated using the forward difference formula. This is so because we are interested with the future propagation of fluid properties given the initial condition (at time $t = 0$). The set of final governing equations involve the first partial derivative with respect to time. Taking $\zeta(t, x)$ to represent some fluid flow variable we have:

$$\frac{\partial \zeta}{\partial t} = \frac{\zeta_j^{k+1} - \zeta_j^k}{\Delta t} \tag{4.3.1}$$

Subscript j corresponds to the j^{th} space node while superscript k corresponds to the k^{th} temporal node.

4.3.2 Spatial Partial Derivative

Partial derivatives with respect to the space co–ordinate y are evaluated using the central difference formula. Since the final set of governing equations involves both the first order and second order partial derivatives, the forms for the variable $\zeta(t,x)$ are given as:

$$\frac{\partial \zeta}{\partial y} = \frac{\zeta_{j+1}^{k} - \zeta_{j-1}^{k}}{2\Delta y}$$
$$\frac{\partial^2 \zeta}{\partial y^2} = \frac{\zeta_{j+1}^{k} - 2\zeta_{j}^{k} - \zeta_{j-1}^{k}}{(\Delta y)^2} \qquad (4.3.2)$$

Again the subscripts and superscripts have the same meaning as they do in section 4.3.1.

4.3.3 Mixed Temporal and Spatial Derivatives

All the flow variables of interest in the current problem involve both temporal and spatial partial derivatives in the same equation. There are known methods for solving such equations. These are the fully explicit method, the fully implicit and the mixed implicit–explicit methods.

The fully explicit method is also known as the forward time central space (FTCS) method while the fully implicit method is also known as the backward time central space (BTCS) method. There are many mixed implicit–explicit methods. The most common and most accurate of the mixed implicit–explicit methods is the Crank–Nicolson scheme.

The BTCS and the Crank Nicolson schemes are independent of the ratio of the time and space width ratios. They are however very difficult to implement with highly coupled and nonlinear systems of equations. Since the final set of

governing equations are highly coupled and non–linear, the FTCS method is preferred in solving the present MHD fluid flow problem.

We next highlight the FTCS method for solving the partial differential equation of the form:

$$\frac{\partial \zeta}{\partial t} = f\left(t, y, \zeta, \frac{\partial \zeta}{\partial y}, \frac{\partial^2 \zeta}{\partial y^2}\right) \tag{4.3.3}$$

Where ζ is the flow variable, t the temporal co–ordinate, y the spatial co–ordinate and f is an arbitrary function in equation (4.3.3).

Given the partial differential equation (4.3.3), the FTCS requires f to be evaluated at the present time level, k (see Figure 4. 2).

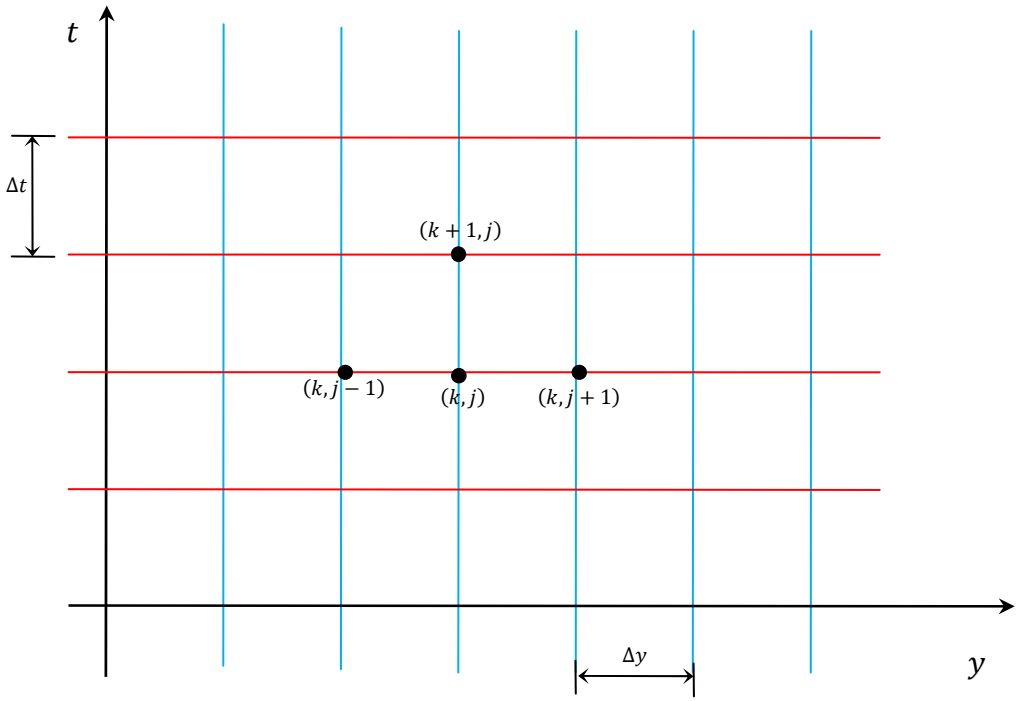

Figure 4. 2: Grid of important points in explicit finite difference method.

With the definition of the time derivative in equation (4.3.1), one writes:

$$\frac{\zeta_j^{k+1}-\zeta_j^k}{\Delta t}=f^k\left(t,y,\zeta,\frac{\partial\zeta}{\partial y},\frac{\partial^2\zeta}{\partial y^2}\right)$$
$$\Rightarrow \zeta_j^{k+1}=\zeta_j^k+\Delta t f^k\left(t,y,\zeta,\frac{\partial\zeta}{\partial y},\frac{\partial^2\zeta}{\partial y^2}\right) \qquad (4.3.4)$$

f^k in equation (4.3.4) implies that all variables in the function f are evaluated at time level k. This method is the easiest to use provided the flow variables are initially known. It is also appropriate for highly non-linear and highly coupled equations since all future variables are determined from already known prior variables. The fully explicit method has a shortcoming in that it is likely to be unstable for large step sizes. This means that the temporal space has to be finely subdivided for convergence. A fine mesh results in many steps and several iterations before convergence.

4.3.4 Finite Difference Equations for the Present Model

The final governing equations as set out in equations (3.8.1), (3.8.2) and (3.8.3) are highly coupled and non–linear. The easiest and most appropriate difference scheme to implement for the system of equations is the explicit method. The system of equations describes the evolution of velocity (both primary and secondary), temperature and concentration. In the subsections that follow we evaluate the finite difference schemes for these fluid properties.

4.3.4.1 Velocity

The velocity along the $x-axis$, $u(t,y)$ is the secondary velocity. Using the finite difference formulas defined in equations (4.3.1) and (4.3.2) and employing the explicit difference method defined by equation (4.3.4) one has:

$$\frac{u_j^{k+1}-u_j^k}{\Delta t}+v_0\frac{u_{j+1}^k-u_{j-1}^k}{2\Delta y}+2Erw_j^k=-\frac{M^2}{1+m^2}\left(mw_j^k+u_j^k\right)+\frac{u_{j+1}^k-2u_j^k-u_{j-1}^k}{\left(\Delta y\right)^2}$$
$$+2\kappa^2\left[y_j\left(\frac{u_{j+1}^k-u_{j-1}^k}{2\Delta y}\right)^2+{y_j}^2\left(\frac{u_{j+1}^k-u_{j-1}^k}{2\Delta y}\right)\left(\frac{u_{j+1}^k-2u_j^k-u_{j-1}^k}{\left(\Delta y\right)^2}\right)\right] \quad (4.3.5)$$

Multiplying through by Δt and using the ratios $r_1=\frac{\Delta t}{\Delta y}$, $r_2=\frac{\Delta t}{\left(\Delta y\right)^2}$ and $r_3=\frac{\Delta t}{\left(\Delta y\right)^3}$ equation (4.3.5) simplifies to:

$$u_j^{k+1}=u_j^k-\frac{v_0r_1}{2}\left(u_{j+1}^k-u_{j-1}^k\right)-2Er\Delta tw_j^k-\frac{M^2\Delta t}{1+m^2}\left(mw_j^k+u_j^k\right)$$
$$+r_2\left(u_{j+1}^k-2u_j^k-u_{j-1}^k\right) \quad (4.3.6)$$
$$+2\kappa^2\left[\frac{r_2}{4}\left(y_j\right)\left(u_{j+1}^k-u_{j-1}^k\right)^2+\frac{r_3}{2}\left(y_j\right)^2\left(u_{j+1}^k-u_{j-1}^k\right)\left(u_{j+1}^k-2u_j^k-u_{j-1}^k\right)\right]$$

For the primary velocity, $w\left(t,y\right)$, the difference equation becomes:

$$\frac{w_j^{k+1}-w_j^k}{\Delta t}+v_0\frac{w_{j+1}^k-w_{j-1}^k}{2\Delta y}-2Eru_j^k=\frac{M^2}{1+m^2}\left(mu_j^k-w_j^k\right)+\left(Gr_L\theta_j^k+Gr_CC_j^k\right)$$
$$+\frac{w_{j+1}^k-2w_j^k-w_{j-1}^k}{\left(\Delta y\right)^2} \quad (4.3.7)$$
$$+2\kappa^2\left[y_j\left(\frac{w_{j+1}^k-w_{j-1}^k}{2\Delta y}\right)^2+{y_j}^2\left(\frac{w_{j+1}^k-w_{j-1}^k}{2\Delta y}\right)\left(\frac{w_{j+1}^k-2w_j^k-w_{j-1}^k}{\left(\Delta y\right)^2}\right)\right]$$

Multiplying equation (4.3.7) through by Δt and using the ratios $r_1=\frac{\Delta t}{\Delta y}$, $r_2=\frac{\Delta t}{\left(\Delta y\right)^2}$ and $r_3=\frac{\Delta t}{\left(\Delta y\right)^3}$ we obtain:

$$w_j^{k+1} = w_j^k - \frac{v_0 r_1}{2}\left(w_{j+1}^k - w_{j-1}^k\right) + 2Er\Delta t\, u_j^k + \frac{M^2\Delta t}{1+m^2}\left(mu_j^k + w_j^k\right) + \Delta t\left(Gr_L\theta_j^k + Gr_C C_j^k\right) + r_2\left(w_{j+1}^k - 2w_j^k - w_{j-1}^k\right) + 2\kappa^2\left[\frac{r_2}{4}\left(y_j\right)\left(w_{j+1}^k - w_{j-1}^k\right)^2 + \frac{r_3}{2}\left(y_j\right)^2\left(w_{j+1}^k - w_{j-1}^k\right)\left(w_{j+1}^k - 2w_j^k - w_{j-1}^k\right)\right] \tag{4.3.8}$$

4.3.4.2 Temperature

For the temperature, $\theta(t, y)$, the difference form of equation (3.8.2) is given as:

$$\frac{\theta_j^{k+1} - \theta_j^k}{\Delta t} + v_0\frac{\theta_{j+1}^k - \theta_{j-1}^k}{2\Delta y} = \frac{1}{Pr}\left(\frac{\theta_{j+1}^k - 2\theta_j^k - \theta_{j-1}^k}{(\Delta y)^2}\right) + Ec\left[\left(\frac{u_{j+1}^k - u_{j-1}^k}{2\Delta y}\right)^2 + \left(\frac{w_{j+1}^k - w_{j-1}^k}{2\Delta y}\right)^2\right] + \frac{EcM^2}{\left(1+m^2\right)^2}\left[\left(mu_j^k - w_j^k\right)^2 + \left(mw_j^k + u_j^k\right)^2\right] \tag{4.3.9}$$

Multiplying equation (4.3.9) through by Δt and using the ratios $r_1 = \frac{\Delta t}{\Delta y}$ and $r_2 = \frac{\Delta t}{(\Delta y)^2}$ we obtain:

$$\theta_j^{k+1} = \theta_j^k - \frac{v_0 r_1}{2}\left(\theta_{j+1}^k - \theta_{j-1}^k\right) + \frac{r_2}{Pr}\left(\theta_{j+1}^k - 2\theta_j^k - \theta_{j-1}^k\right) + \frac{Ecr_2}{4}\left[\left(u_{j+1}^k - u_{j-1}^k\right)^2 + \left(w_{j+1}^k - w_{j-1}^k\right)^2\right] + \frac{EcM^2\Delta t}{\left(1+m^2\right)^2}\left[\left(mu_j^k - w_j^k\right)^2 + \left(mw_j^k + u_j^k\right)^2\right] \tag{4.3.10}$$

4.3.4.3 Concentration

For the concentration $C(t, x)$ the difference form of equation (3.8.3) is given as:

$$\frac{C_j^{k+1} - C_j^k}{\Delta t} + v_0\frac{C_{j+1}^k - C_{j-1}^k}{2\Delta y} = \frac{1}{Sc}\left(\frac{C_{j+1}^k - 2C_j^k - C_{j-1}^k}{(\Delta y)^2}\right) \tag{4.3.11}$$

Upon multiplying equation (4.3.11) through by Δt and using the ratios $r_1 = \frac{\Delta t}{\Delta y}$ and $r_2 = \frac{\Delta t}{(\Delta y)^2}$ one obtains:

$$C_j^{k+1} = C_j^k - \frac{v_0 r_1}{2}\left(C_{j+1}^k - C_{j-1}^k\right) + \frac{r_2}{Sc}\left(C_{j+1}^k - 2C_j^k - C_{j-1}^k\right) \qquad (4.3.12)$$

Equations (4.3.6), (4.3.8), (4.3.10) and (4.3.12) are the difference forms of the secondary velocity, primary velocity, temperature and concentration. In this form they can be solved using a computer to obtain solutions at successive time levels.

4.4 Computer Program

A computer program written in `matlab` (Appendix II) was used solve the difference equations. The initial and boundary conditions were set as given in relations (3.8.4) with $y = \infty$ set as $y = 4$. The program has graphical outputs for the primary and secondary velocity profiles, temperature profiles and concentration profiles for various fluid parameter values. In the next chapter these results are presented and discussed.

CHAPTER FIVE

RESULTS AND DISCUSSION

5.1 Overview

In this chapter we present the numerical results obtained upon employing the program mentioned in section 4.4. The trends observed upon varying various fluid properties are discussed and explained. First the general trend is presented in a mesh plot where all the fluid properties are maintained at default values. We then present the trends as each fluid property is varied at time $t = 0.2$ while maintaining other properties at default values. Last, we present the trends at various specific times while all the fluid properties are set to default values.

5.2 Fluid Property Default Values

Since the problem has been non-dimensionalized, there is no justification for any particular choice of the default values of the fluid properties. Of interest is how changes in these properties affect the flow variables. The choice made for default values of fluid properties are:

$$Pr = 0.71,\ \ Gr_L = 1,\ \ Gr_C = 1,\ \ Ec = 1,\ \ Sc = 2.5,\ \ M^2 = 1,\ \ m = 0.1,\ \ Er = 1,\ \ v_0 = 0.5 \tag{5.2.1}$$

5.3 Three Dimensional Plots

Since the flow variables were all functions of spatial dimension, y, and temporal dimension, t, we obtained mesh plots for all the variables. The mesh plots give a general trend of the spatial bifurcation and the temporal evolution of the flow variables.

From Figure 5. 1 one notes that the primary velocity falls from unit to zero along the $y-coordinate$ initially very fast but more slowly as time increases. Similar observations are made for the temperature and concentration profiles. This is in agreement with the initial and boundary conditions that require that primary velocity, temperature and concentration be instantaneously raised to unit at the plate ($y=0$) and maintained at zero at the free flow region ($y=\infty$). With time the flow variables are transmitted to the boundary layer of the fluid, hence the sequential fall in the flow variables. The secondary velocity, on the other hand, increases from zero to a maximum value, then falls back to zero again as the initial and boundary conditions require. The increase in secondary velocity is attributed to the gain in kinetic energy. Sequential gain in this kinetic energy leads to the profile observed.

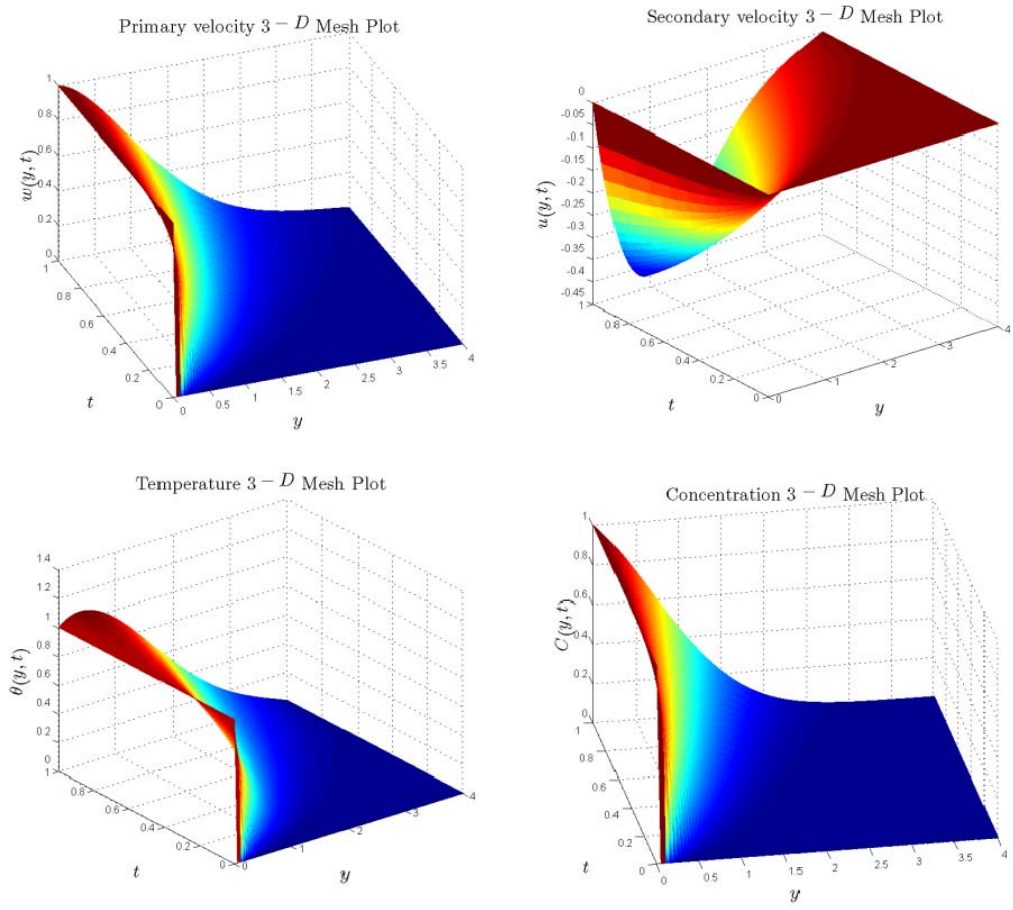

Figure 5. 1: Three dimensional mesh plots for the four flow variables.

5.4 Effect of Prandtl Number

While keeping all the other fluid properties at their default values, the Prandtl number was varied as $Pr = 0.71, 1, 3, 5 \; and \; 7.1$. The results obtained are presented in Figure 5. 2 below.

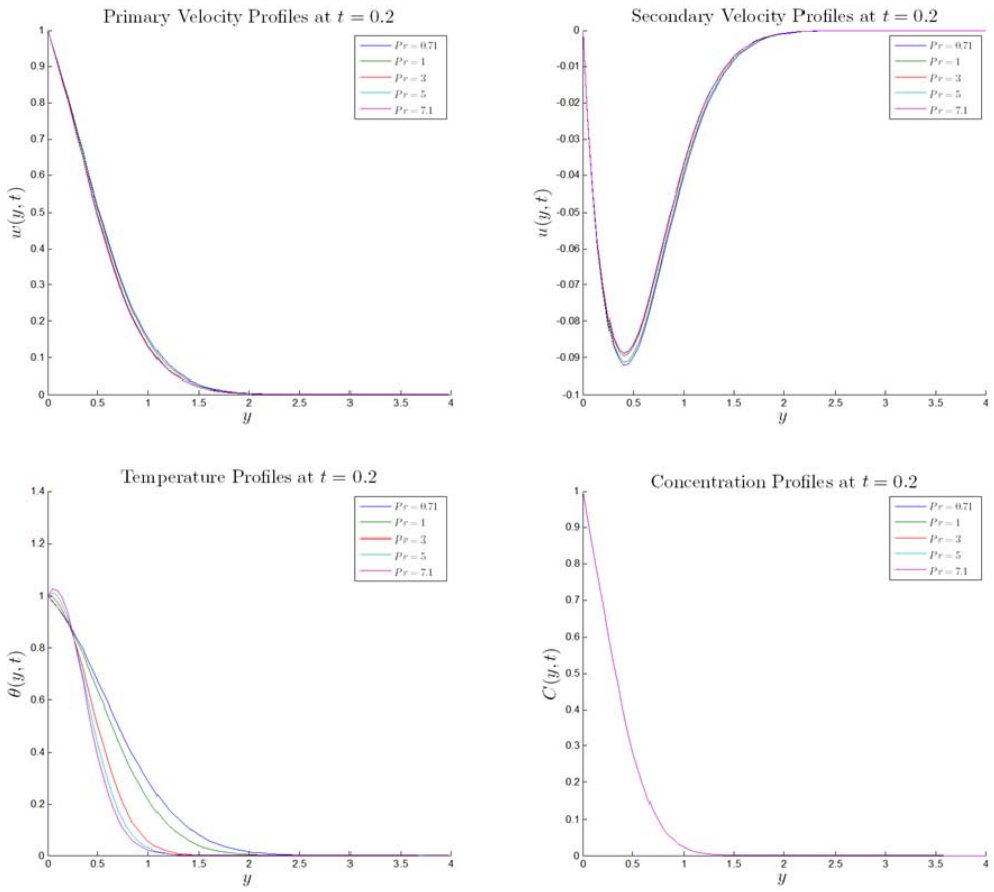

Figure 5. 2: Fluid flow profiles for various Prandtl numbers. Other properties kept at default.

It is observed that increase in Prandtl number leads to a slight decrease in both primary and secondary velocities. Except for very small region near the plate, the temperature, too, decreases more sufficiently with increase in the Prandtl number. The effect of Prandtl number on concentration is diminished.

These observations are a direct consequence of equations (3.8.1), (3.8.2) and (3.8.3). From these equations, there is an inverse relationship between the energy

equation and the Prandtl number. This results in the more pronounced effect of the Prandtl number on the temperature profile. Temperature then affects the primary velocity which in turn affects the secondary velocity. This leads to the slight effect of Prandtl number on both primary and secondary velocity profiles. Neither temperature nor the Prandtl number affects the concentration equation and hence the diminished effect on the concentration profile.

Physically, the Prandtl number is the relative diffusivity of momentum to that of heat. This implies that small values of Prandtl number imply that heat diffuses very fast relative to the fluid velocity e.g. in liquid metals. For higher values of Prandtl numbers, heat diffuses relatively slowly when compared to velocity e.g. in oils. Hence the decrease in thermal and consequently the velocity boundary layers as the Prandtl number increases. There is little effect on mass transfer (concentration) by the Prandtl number.

5.5 Effect of Thermal Variant of Grashof Number

While maintaining all other fluid properties at their default values, the thermal variant of Grashof number was varied as $Gr_L = -2, -1.5, -1, -0.5, 0.1, 1, 1.5, 2$.

From Figure 5. 3, it is observed that both primary and secondary velocities are substantially affected by the Grashof number. Increase of the negative Grashof number leads to decrease in both primary and secondary velocities. Increase in the positive Grashof number leads to increase in both the primary velocities. The temperature profile is only slightly affected by the Grashof number with observations similar to those of velocity profiles. Again, concentration is, apparently, unaffected by the Grashof number.

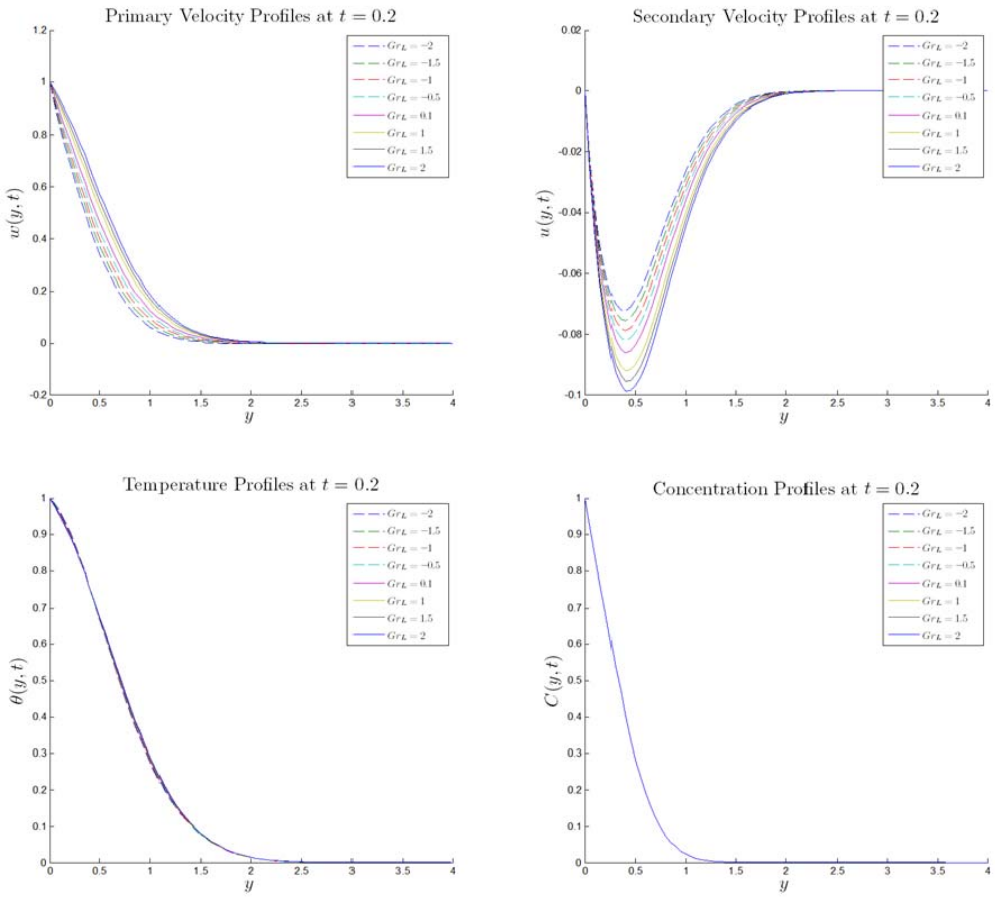

Figure 5. 3: Fluid flow profiles for various thermal Grashof numbers. Other properties kept at default values.

The trends above can be explained from equations (3.8.1) where Gr_L affects the primary velocity which in turn affects the secondary velocity. Therefore the primary velocity is affected more prominently by the thermal variant of Grashof number. Due to the relationship between primary and secondary velocity, the secondary velocity is also affected by Gr_L but by a smaller factor. The slight effect on the temperature profiles is a consequence of the relationship between the primary and secondary velocity in equation (3.8.2).

Physically, the thermal variant of Grashof number is a derivative of buoyancy effects. According to Archimedes' principle, less dense substance will be displaced by the heavier substance. The heated fluid expands and its density

reduces. The heavier fluid sinks to displace this lighter fluid and hence the increased primary velocity. The secondary velocity increases too due to the rotary motion of the fluid coupled with Hall effects. Increase in fluid velocity implies increase in kinetic energy which ultimately results in increase in thermal agitation (temperature). Concentration gradient is unaffected since these changes are not in the concentration gradient coordinate.

5.6 Effect of Concentration Variant of Grashof Number

Varying the concentration variant of Grashof number as $Gr_C = 1, 1.5, 2, 4$, while keeping the other fluid properties at their default values, we obtained the results in Figure 5. 4.

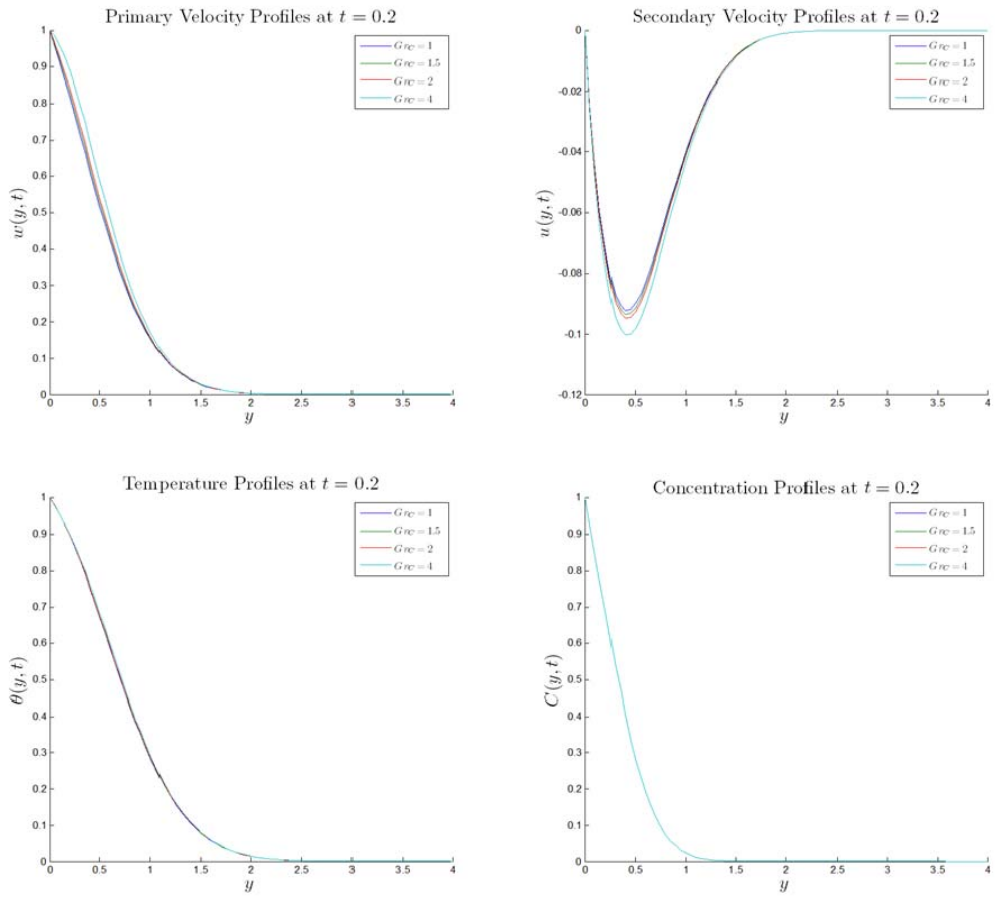

Figure 5. 4: Flow profiles for various concentration Grashof numbers. Other fluid properties kept at default.

It is observed that increase in the concentration variant of the Grashof number increases the primary velocity, secondary velocity and the temperature. Observed increase is larger for the primary velocity than for secondary velocity and temperature. There is no observable effect on the concentration profiles.

It is clear from equations (3.8.1), (3.8.2) and (3.8.3) that there is a direct relationship between the primary velocity and the concentration variant of Grashof number. An increase in the concentration Grashof number will lead to an increase in the primary velocity. From the relationship between the primary and secondary velocities, an increase in primary velocity will also lead to an increase in secondary velocity. The temperature equation contains terms with both primary and secondary velocity. Therefore, increases in primary and secondary velocities will result in an increase in temperature. However, increases in secondary and temperature are minimal compared to the increases in primary velocity. This is because there is no direct relationship between the two flow variables and the concentration variant of the Grashof number. There is no observable effect on the concentration gradient since there is no mathematical relationship between the concentration variant of Grashof number and the concentration gradient.

Physically, concentration refers to the presence of a given species in a sample. This presence can affect the buoyancy effects in that the expected displacement may be enhanced or inhibited. If the species on top of the heated and expanding volume is denser then the primary velocity will be enhanced. If, however, the species at the top will be lighter then buoyancy will be inhibited. The enhancement of buoyancy leads to increased primary and secondary velocities. This leads to increased kinetic energy and hence thermal excitation. The effect on

the concentration gradient and the concentration variant is minimal as the direction of flow due to buoyancy does not affect the concentration gradient.

5.7 Effect of Eckert Number

Varying the Eckert number as $Ec = 0.1, 0.5, 1, and\ 1.5$, while keeping the other fluid properties at their default values, yields the results in Figure 5. 5. From the graphs, we observe that the Eckert number only slightly affects the primary and secondary velocities by increasing them marginally. The increase in temperature is more appreciable but there is no observable effect on the concentration gradient.

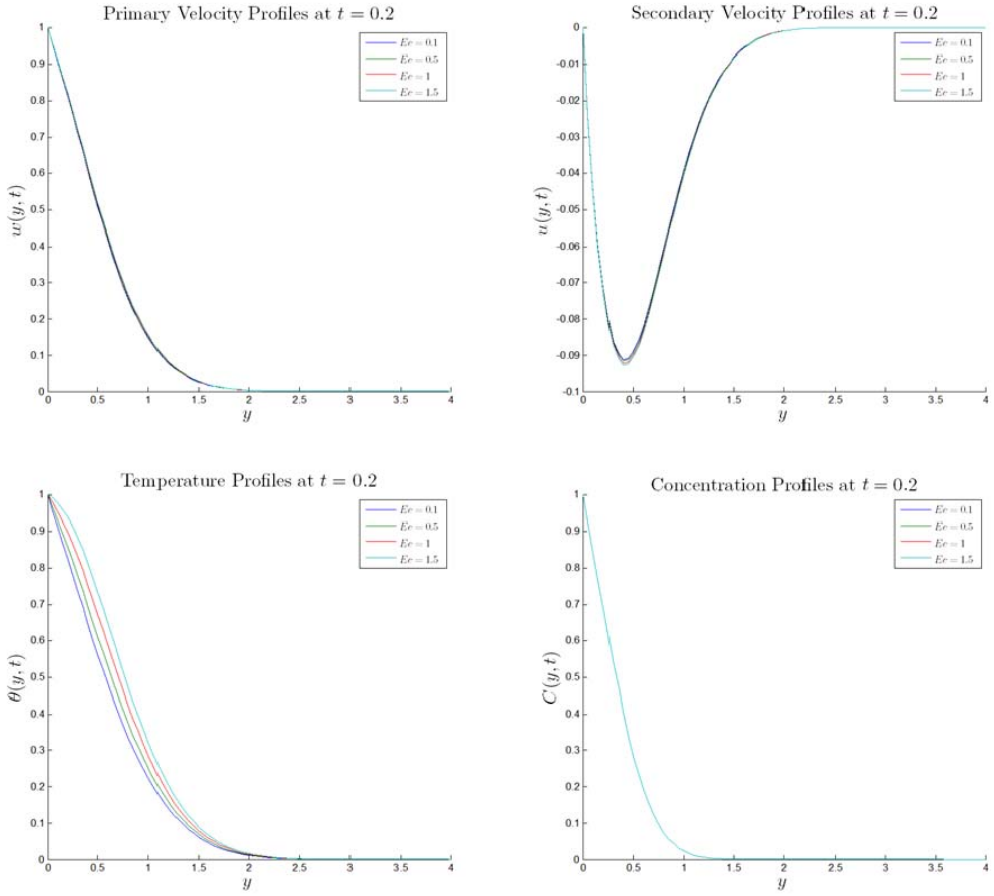

Figure 5. 5: Flow profiles for various Eckert numbers. Other fluid properties are kept at their default values.

The Eckert number affects the temperature profiles the most because from equation (3.8.2) the Eckert number directly affects the energy equation. There is a

notable slight increase in the primary velocity when the Eckert number increases because of the entry of temperature into the equation of motion, (3.8.1). Therefore increase in primary velocity is a carryover effect from temperature. The increase in secondary velocity is also due to the relationship between the primary and secondary velocities, a carryover effect. There is no notable effect on the concentration profiles since there is a very remote relationship between the Eckert number and the concentration gradient implied by equation (3.8.3).

Physically, the Eckert number is a ratio of kinetic energy to the enthalpy. This means that a large Eckert number implies more kinetic energy and reduced temperature difference. Kinetic energy increase and reduced temperature difference implies that more heat transfer and hence the rise in temperature profiles. A rise in temperature leads to more agitation and hence the marginal increases in both primary and secondary velocity profiles. These changes in enthalpy and kinetic energies do not translate to mass transfer effects and hence very little effect on the concentration profiles.

5.8 Effect of Schmidt Number

By maintaining other fluid properties at their default values and varying the Schmidt number as $Sc = 2, 2.5, 5, 10$, we obtained the results shown Figure 5. 6. We observed that the Schmidt number affects mostly the concentration profiles and affects the primary and secondary velocity minimally. There is no observable effect on the temperature profiles. Increase in the Schmidt number inhibits the primary and secondary velocities and the concentration profiles.

Mathematically, these observations can be explained from the relations in equations (3.8.1), (3.8.2) and (3.8.3). We notice that there exists an inverse

relationship between the concentration and the Schmidt number, therefore the inhibition of the concentration profile on increasing the Schmidt number. The effect on the primary and secondary velocities is due to the carryover effect where the primary velocity is affected by the concentration and the secondary velocity by the primary velocity. The temperature profile is seemingly unaffected due to the remoteness of the relationship between it and the Schmidt number.

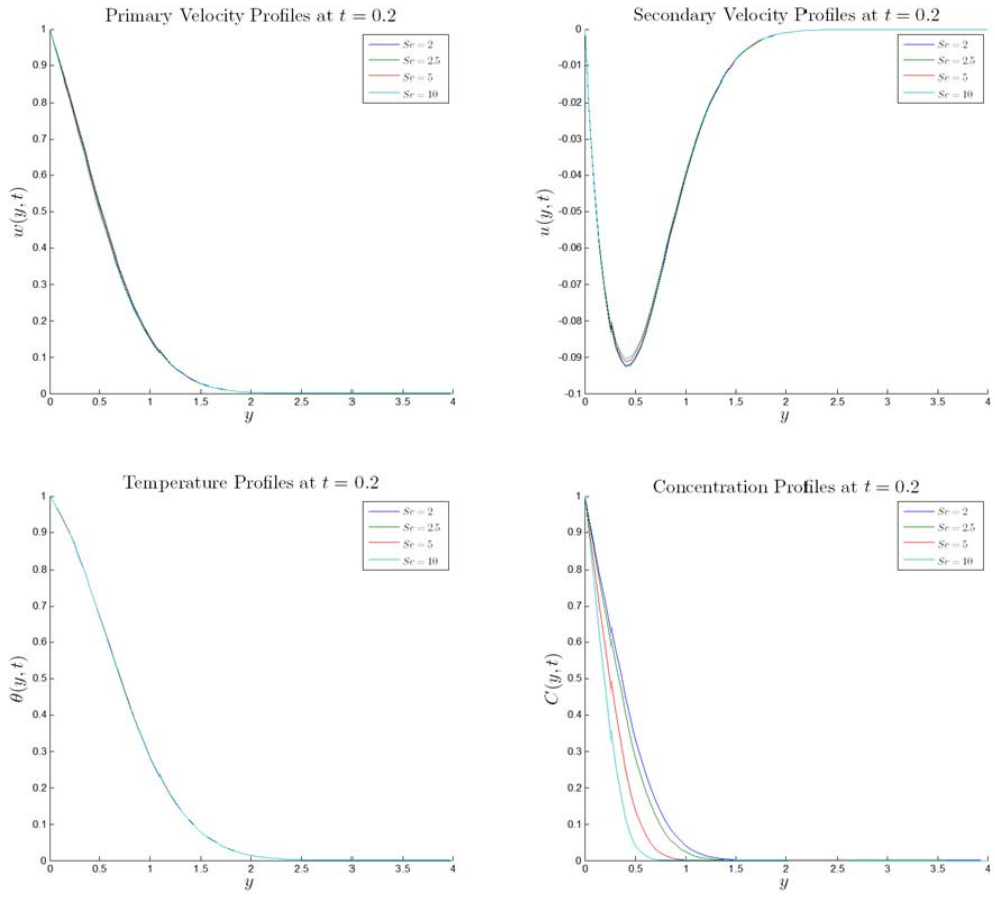

Figure 5. 6: Flow profiles for various Schmidt numbers. Other fluid properties were maintained at their default values.

The Schmidt number physically represents the ratio of the momentum diffusivity to mass diffusivity. This implies that a higher Schmidt number results in a thicker velocity boundary layer than the concentration boundary layer. This therefore inhibits concentration profiles. Inhibiting concentration profiles in turn affects the buoyancy and hence primary velocity profiles. The secondary velocity profiles are

affected due to the rotary motion of the fluid. Reduced kinetic energy will remotely affect the temperature profiles.

5.9 Effect of Magnetic Parameter

The magnetic parameter, M^2, was varied as $M^2 = 1, 5, 10, 20, 50$, while other fluid properties were maintained at their default values. The results obtained are as shown in Figure 5. 7.

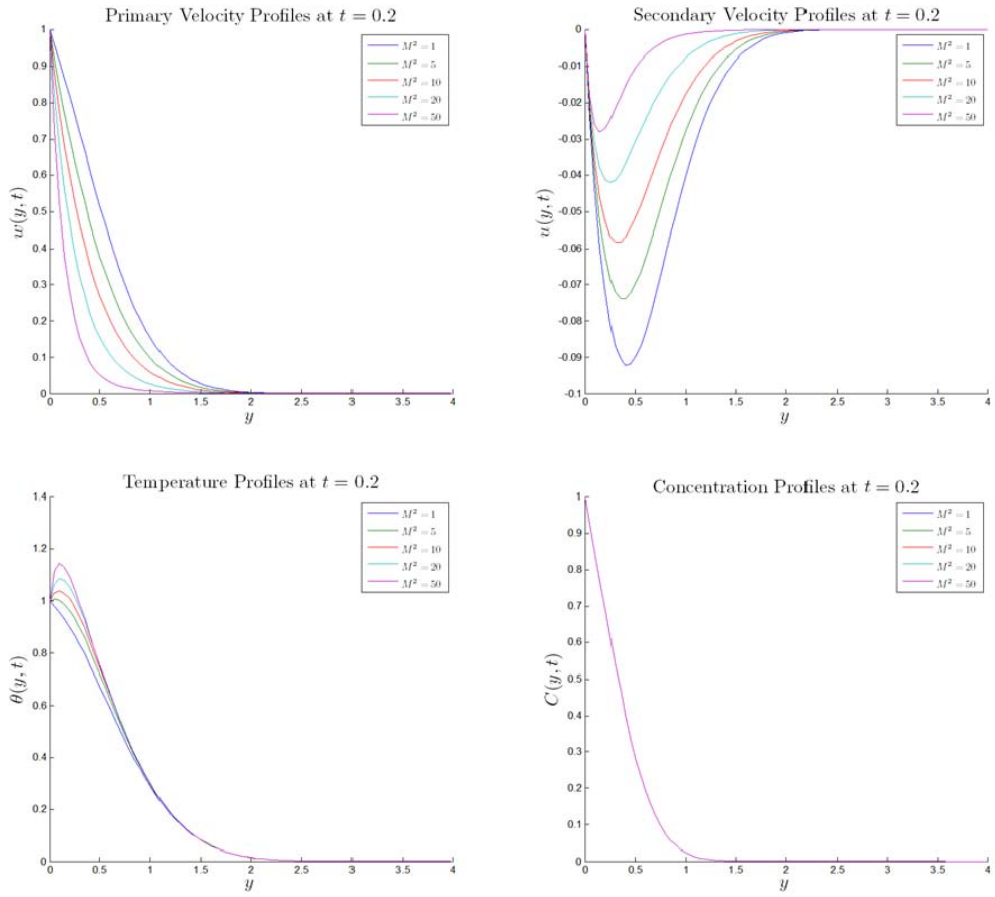

Figure 5. 7: Flow profiles for various magnetic parameter values. Other fluid properties were maintained at their default values.

It is observed that the magnetic parameter affects the both primary and secondary velocities and temperature profiles. The magnetic parameter inhibits both velocities but enhances temperature build up. There is no observable effect on the concentration profiles.

The above observations are as a result of the final set of governing equations, (3.8.1), (3.8.2) and (3.8.3). It can be deduced from the set of equations that the magnetic parameter has an inhibitive effect on both primary and secondary velocities while having a positive effect on the temperature. The relationship between the concentration gradient and the magnetic parameter is distant.

Physically, the magnetic parameter is a measure of the magnetic field strength within the fluid. It actually represents the ratio of the electromagnetic force to viscous forces. Higher magnetic field strength coupled with Joule's heating enhances turbulence and hence the build up of heat. Higher magnetisation leads to larger values of Lorentz force which inhibits both primary and secondary velocities. There is, however, little correlation between the magnetic parameter and mass transfer.

5.10 Effect of Hall Parameter

While maintaining the other fluid properties at their default values, the Hall parameter was varied as $m = 0.1, 0.5, 1, 2$. The results obtained are as shown in Figure 5. 8. It is observed that the Hall parameter has marginal effects on the both velocity profiles and temperature profiles. While an increase in the Hall parameter leads to an enhancement of the velocity profiles, it is interesting to note that it has the reverse effect on the temperature profiles. There is, apparently, no effect on the concentration profiles.

One can deduce, mathematically, the above observations from the final set of governing equations. From equations (3.8.1) and (3.8.2) the parameter, m, is combined with other parameters with the net negation effect on the two velocity

profiles and a net additional effect on the temperature profiles. There is no direct correlation between the concentration profiles and the Hall parameter.

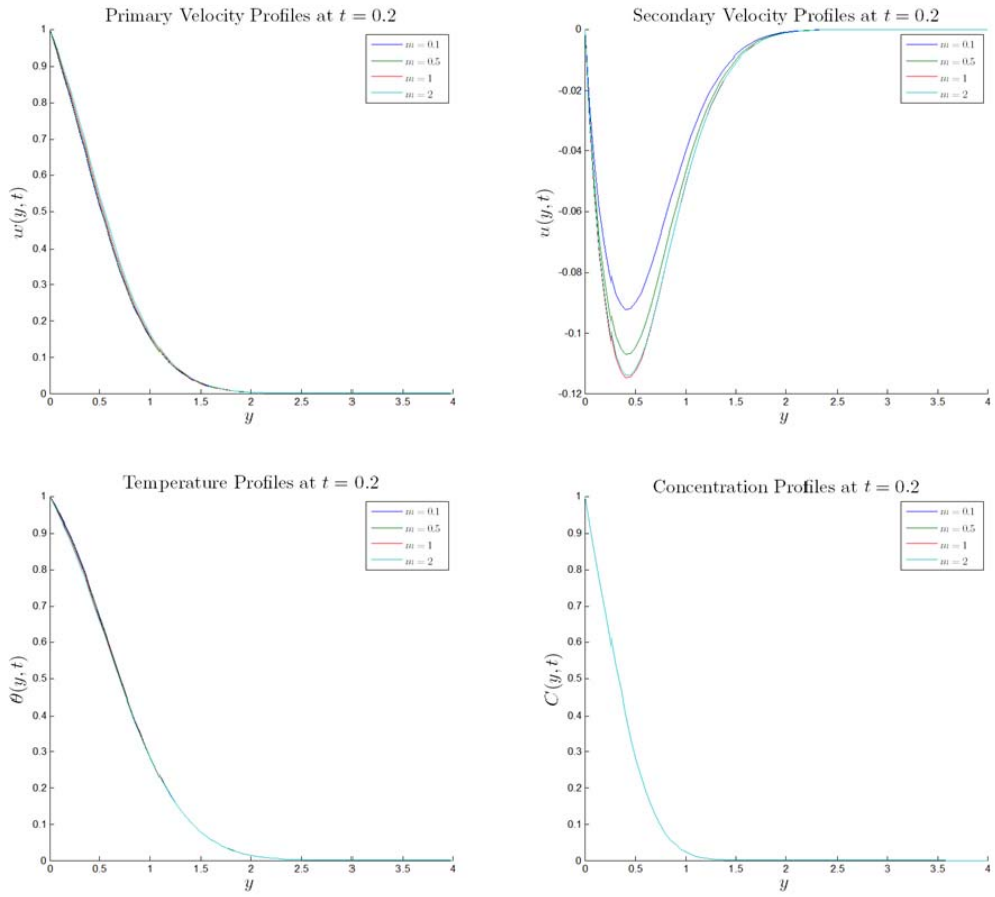

Figure 5. 8: Flow profiles for various Hall parameter values. Other flow properties are maintained at their default values.

The Hall parameter has the physical rotary effect. This is because Hall currents are developed in cyclotrons. The effect of this is to increase the primary velocity and most often the secondary velocity. The rotational motion of the fluid particles will draw energy from the system and hence reduce thermal agitation. The rotation, being vertical, does not affect mass transfer within the fluid.

5.11 Effect of Rotational Parameter

The rotational parameter was varied as $Er = 1, 2, 3, 4$, while the other fluid properties were maintained at their default values. The results obtained are as shown in Figure 5. 9.

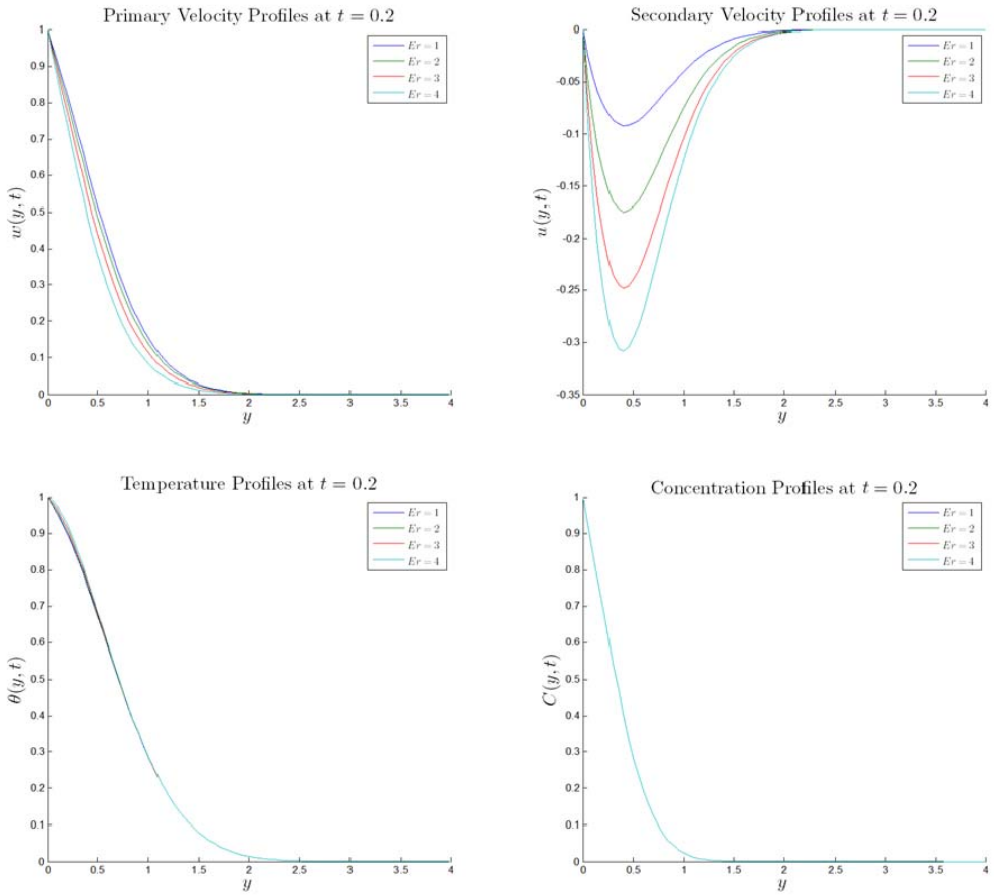

Figure 5. 9: Flow variables for various rotational parameters. Other fluid properties are maintained at their default values.

The rotational parameter is observed to have a suppressing effect on the primary velocity while reinforcing the secondary velocity profiles. The rotational parameter also enhances the temperature profiles but seems to have no observable effect on the concentration profiles.

The observations above are a result of equations (3.8.1), (3.8.2) and (3.8.3). The rotational parameter has a negative effect on the primary velocity but has a

positive effect on the secondary velocity profiles. The marginal effect on the temperature profiles is attributed to the carryover effect from both the primary and secondary velocities. There is little conceivable correlation between the concentration profiles and the rotational parameter.

Physically, the temperature rises due to the increased turbulence enhanced by rotation. The primary velocity decreases because rotation transfers some of the primary velocity to secondary velocity which increases. There being distant correlation between the concentration profiles and the rotation parameter, there can be no noticeable change in the concentration profiles.

5.12 Effect of Mass Transfer Velocities

The injection $(+)$ or suction $(-)$ velocity, v_0, was varied as $v_0 = -0.5, -0.25, 0.25, 0.5$. Other fluid properties were maintained at their default values as set in relations (5.2.1). The results obtained are as shown in Figure 5. 10.

It is observed that the injection velocities have a reinforcing effect on all the flow variables while the suction velocities have a suppressing effect on all the flow variables. Mathematically, this is a result of the incrementing effect that v_0 has on all the final governing equations. Physically injection transfers the wall properties to the fluid within the boundary layer. The faster the rate of injection the faster the transfer of wall characteristics is. This leads to the enhancement of the primary velocity, temperature and concentration profiles. The secondary velocity is enhanced too because of the rotational system of motion.

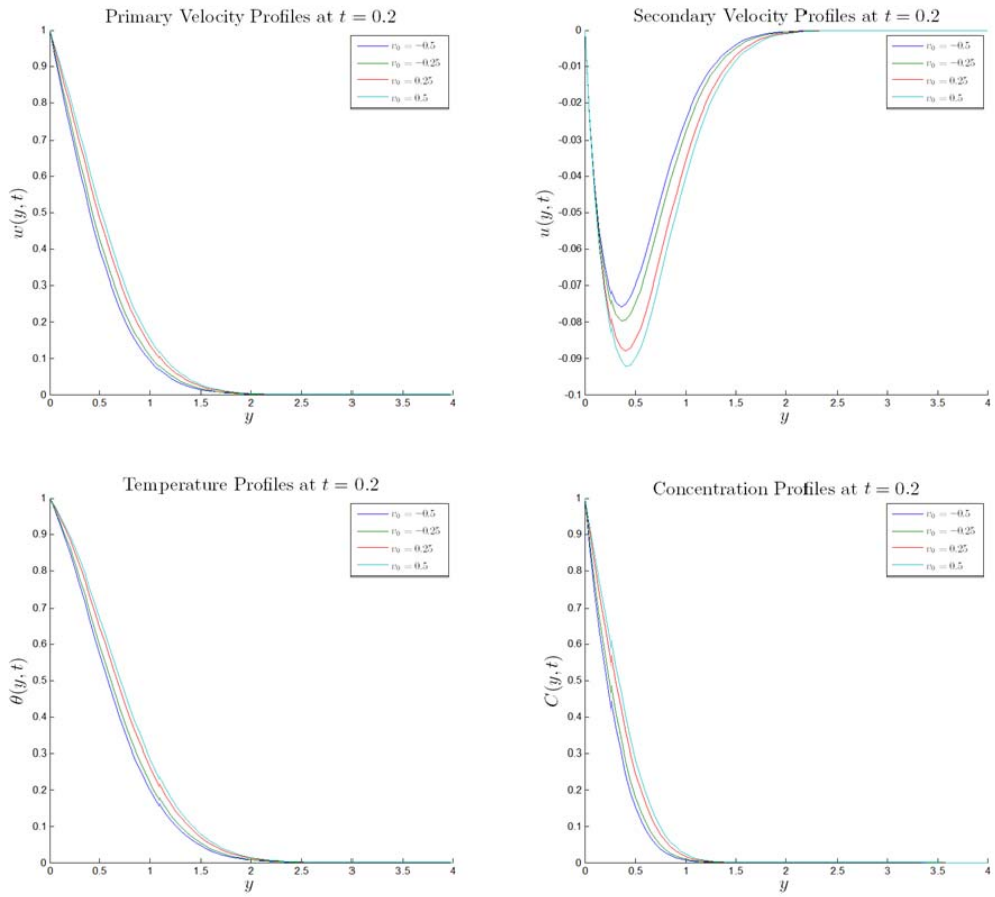

Figure 5. 10: Flow profiles for various mass transfer velocities. Other fluid properties are maintained at their default values.

5.13 Time Evolution of the Flow Variables

Last the effect of the time evolution of the profiles is considered. Time was varied as $t = 0.2, 0.4, 0.6, 0.8$. The results obtained are presented in Figure 5. 11.

It is observed that with time all the profiles are enhanced. This implies that at time $t = \infty$ we expect all the plate properties to have been transmitted throughout the boundary layer. This is physically expected since the plate flow properties are constant. As time goes by, more and more of the plate flow properties are transmitted onto the boundary layer. This results in successive build–up of all the flow variables.

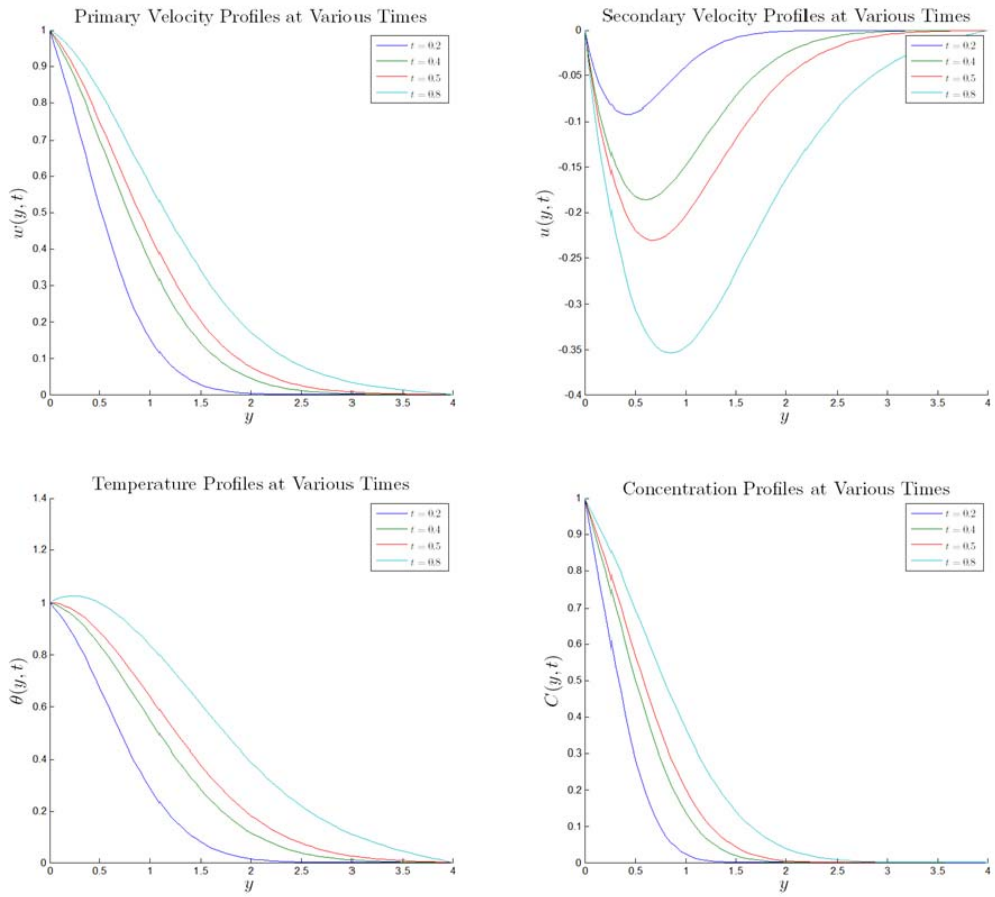

Figure 5. 11: Flow profiles at various times keeping all the fluid properties at their default values.

CHAPTER SIX

CONCLUSION AND RECOMMENDATIONS

6.1 Conclusion

In the present approach we were able to mathematically formulate a suitable model to solve the magnetohydrodynamic turbulent flow past an infinite vertical porous plate in a rotating medium. A computer program was written in matlab to solve the highly coupled and nonlinear partial differential equations. The impact of various fluid properties on the primary velocity, secondary velocity, temperature and concentration were discussed.

The results obtained in the present problem closely compared with those of Das *et al* (2011) and Mutua *et al* (2013). Although Das used the multi–parameter perturbation and the fact that our system was rotating, most observations he drew agreed with ours. Mutua used a finite difference method just like the present one only in a different programming language. His problem differed with the present one in that our system was porous and he considered a varying magnetic field. Even so, most of the results they obtained agreed closely with the present ones. This agreement with other results is encouraging.

Joule's heating, mass transfer, rotation and Hall current have a profound effect on almost all flow variables. Some of these effects have initially been assumed to be of negligible effect but accounting for them in the present model shows that they result in a substantive effect. Concentration profile was the least affected by most of the fluid properties considered. This is due to the fact that concentration

gradient diffuses along the $y-axis$ and could only be affected by the Schmidt number and injection or suction velocities.

The results reported in the present model are in a good agreement with general trends. This follows the physical expectation of the effect of various parameters. As discussed in chapter five physical trends were eminent in the results. Some results like the magnetic parameter on temperature profiles is very interesting. Increase in M^2 yielded increase in temperature profiles. This is a consequence of the Joule's heating effect.

In the world we live in today, a great concern is how to generate green energy. With the universe full of charged particles, the study of magnetohydrodynamics can provide a future source of electricity. Further with population expected to exceed the resources, scientists are in a rush to find alternatives outside earth to colonise. One of the problems faced to occupy neighbouring planets like Mars is the atmosphere. Electromagnetic control of the atmosphere has been theoretically suggested as a possible solution. The thinning of the ozone layer can be retarded by magnetohydrodynamic excitation.

6.2 Recommendations

The success of this method in yielding results that are in good agreement with previous studies and general trends has led us into making the following recommendations.

(i) The model to be extended to include ion slip currents

(ii) The approach to be extended to solve similar problem with varying magnetic field strength

(iii) A generalisation to be made by including a porosity factor and other similar factors for inclusion of Hall currents and rotation

(iv) The magnetic field to be inclined at an angle

REFERENCES

Alfvén, H. (1942). *Existence of electomagnetic-hydrodynamic waves*. Nature, vol. 150, pg. 405-406

Calvert, J. B. (2002). *Magnetohydrodynamics: The Dynamics of Conducting Fluids in Electromagnetic Fields.* http://mysite.du.edu/~jcalvert/phys/mhd.htm

Chaudhar, R. C. and Jain A. (2006). *Combined Heat and Mass Transfer Effects on MHD Free Convection Flow past an Oscillating Plate Embedded in Porous Medium*. Romanian Journal of Physics vol. 52, issue 5, pg. 505-524.

Das, S. S., Biswal S. R., Tripathy U. K. and Das P. (2011). *Mass Transfer Effects on Unsteady Hydromagnetic Convective Flow past a Vertical Porous Plate in a Porous Medium with Heat Source*. Journal of Applied Fluid Mechanics vol. 4, issue 4, pg. 91-100.

Das, S. S., Satabathy A., Das J. K. and Sahoo S. K. (2007). *Numerical Solution of Unsteady Free Convective MHD Flow past an Accelerated Vertical Plate with Suction and Heat Flux.* Journal of Ultra Scientist of Physical Sciences vol. 19, issue pg. 105-112.

Del Sordo, F., Guerrero, G. and Brandenburg A. (2013). *Turbulent Dynamos with Advective Magnetic Helicity Flux*. Monthly Notices of the Royal Astronomical Society vol. 429, issue 2 pg 1686-1694

Ghosh, S and Ghosh A. K. (2008). *On Hydromagnetic Rotating Flow of a Dusty Fluid near a Pulsating Plate.* Computational and Applied Mathematics vol. 27, issue 1, pg. 1-30.

Greenspan, H. P. and Howard L. N. (1963). *Unsteady Rotating Flow past an Impermeable or Permeable Plate*. Applied Science Research Section vol. 17, pg. 385.

Gupta, A. S. and Soundalgekar, V. M. (1975) *On Hydromagnetic Flow and Heat Transfer in a Rotating Fluid past an Infinite Porous Wall*. Zeitschrift fuer Angewandte Mathematik und Mechanik, vol. 55, pg. 762-764.

Hartmann, J. (1937). *Theory of the laminar flow of an electrically conductive liquid in a homogeneous magnetic field*. K. Dan. Vidensk. Selsk. Mat. Fys. Medd. Vol. 15, issue 6, pg. 1–28.

Incropera, F. P. and Dewitt, D.P. (1885). *Fundamentals of Heat and Mass Transfer*. John Wiley and Sons Inc.

Hasimoto, H. (1957). *Boundary Layer Growth on a Flat Plate with Suction or Injection*. Journal of Physical Society 0f Japan vol. 12, pg 68-72.

Hughes, J. and Gaylord J. S. (1964). *Four Equation Turbulence Model for Prediction of the Turbulent Boundary Layer Affected by Buoyancy Force over a Flat Plate*. International Journal of Heat and Mass Transfer vol. 27, pg. 2387-2395.

Kinyanjui, M., Chartuvedi N. and Uppal S. M. (1998). *MHD Stokes Problem for a Vertical Infinite Plate in a Dissipative Rotating Fluid with Hall Current*. Energy Conversion Management vol. 39, issue 5/6, pg. 541-548

Kwanza, J. K., Kinyanjui M. and Uppal S. M. (2003). *MHD Stokes Free Convection Flow past an Infinite Vertical Porous Plate Subjected to a Constant Heat Flux with Ion Slip Current and Radiation Absorption*. Far East Journal of Applied Mathematics vol. 12, issue 2, pg. 105-131.

Makinde, O. D., Mango J. M. and Theuri D. M. (2003). *Unsteady Free Convection Flow with Suction on an Accelerating Porous Plate*. AMSE Journal of Modelling Measurement and Control B vol. 72, issue 3, pg. 39-46.

Mansuti, D., Pontrelli G and Rajagopal K. R. (1993). *Steady Flows of Non–Newtonian Fluids past a Porous Plate with Suction or Injection*. International Journal for Numerical Methods for Fluids vol. 17, pg. 927-941.

Marigi, E. M., Kinyanjui, M. and Kwanza, J.K. (2012). *Hydromagnetic Turbulent Flow past a Semi-Infinite Vertical Plate Subjected to Heat Flux*. The International Institute for Science, Technology and Education vol. 2, pg 15-25.

McComb, W. D. (1990). *The Physics of Fluid Turbulence*. Oxford University Press.

Mutua N., Kinyanjui M. and Kwanza J. (2013). *Stoke's Problem of a Convective Flow past a Vertical Infinite Plate in a Rotating System in Presence of Variable Magnetic Field.* International Journal of Applied Mathematics Research vol. 2, issue 3, pg. 5-11.

Prandtl, L. (1904). *On the motion of fluids of very small visicosity*. Verh. III. Intern. Math. Kongr., Heidelberg, S. 484–491

Schaschke, C. (1998). *Fluid Mechanics: Worked Examples for Engineers. 1st Ed*. Institution of Chemical Engineers.

Schilschting, H. (1979). *Boundary Layer Theory*. Journal of Applied Mathematics and Mechanics vol. 60 issue 4 pg. 217

Schnack, D. D. (2009). *Lectures in Magnetohydrodynamics with an Appendix on Extended MHD*. Lecture Notes in Physics vol. 780. Springer, Berlin Heidelberg.

Serway, R.A., Jewett, J.W. (2004). *Physics for scientists and engineers. 6th ed*. Thomson Brooks/Cole.

Sharma, P. R. and Pareek D. (2002). *Steady Free Convection MHD Flow past a Vertical Porous Moving Surface*. Indian Journal of Theoretical Physics vol. 50, pg 5-13.

Versteeg H. K. and Malalasekera W. (2007). *An Introduction to Computational Fluid Dynamics*. Pearson Education Limited.

APPENDICES

Appendix I: Publications

1. Mayaka, J. O., Sigey, J. K. and Kinyanjui, M. (2014). *MHD Turbulent Flow in a Porous Medium with Hall Currents, Joule's Heating and Mass Transfer*. International Journal of Science and Research vol. 3 issue 8 pg. 73–83. http://www.ijsr.net/archive/v3i8/MDIwMTUxNTk=.pdf

Appendix II: Program for the MHD Problem

```
1
2   function mhdproblem()
3   clear all;
4   clc
5
6   %CONSTRUCTION OF THE GRID IN y AND t
7   %Generate array y values
8   N = 81;
9   y1 = 0;
10  yN = 4.0;
11  dy = (yN-y1)/(N-1);
12  y = zeros (1, N);
13  for j=1:N
14      y(j) = (j-1)*dy;
15  end
16  %y%Test output for y values. Remove the earlier comment to see
17  values.
18
19  %Generate array t values
20  K = 80001;
21  t1 = 0;
22  tK = 1;
23  dt = (tK-t1)/(K-1);
24  t = zeros (1, K);
25  for k=1:K
26      t(k) = (k-1)*dt;
27  end
28  %t%Test output for t values. Remove the earlier comment to see
29  values.
30
31  %DECLARING CONSTANTS
32  PR = 0.71;%Prandtl number:{0.71},1,3,5,7.1
33  GRL = 1;%Grashoff number:-2,-1.5,-1,-0.5,0.1,{1},1.5,2
34  GRC = 1;%Grashoff number variant for concentration:{1},1.5,2,4
35  EC = 1;%Eckert number:0.1,0.5,{1},1.5
36  SC = 2.5;%Schmidt number:2,{2.5},5,10
37  SQUAREDM = 1;%Magnetic parameter/Hartman number:{1},5,10,20,50
38  em = 0.1;%Hall parameter:{0.1},0.5,1,2
39  ER = 1;%Rotational parameter:{1},2,3,4
40  vnought = 0.5;%Drift velocity in the y-direction:-0.5,-
41  0.25,0.25,{0.5}
42  kappa = 0.4;%Karman constant
43
44  %SETTING THE BOUNDARY CONDITIONS
45  u = zeros (K, N); w = zeros (K, N); theta = zeros (K, N);...
46      C = zeros (K, N);%Initial conditions at t<0
47  u(1:K,1) = 0; w(1:K,1) = 1; theta(1:K,1) = 1; C(1:K,1) =
48  1;%Boundary...
49
50  %conditions at y=0
51  u(1:K,N) = 0; w(1:K,N) = 0; theta(1:K,N) = 0; C(1:K,N) =
52  0;%Boundary...
53                                                  %conditions at
54  y=4(infinity)
55  for j = 2:N-1
56      u(1,j) = 0; w(1,j) = 0; theta(1,j) = 0; C(1,j) = 0;%Initial...
```

```
                                                        %conditions
at t = 0
end

%COMPUTATION OF VARIABLES
r1 = dt/dy; r2 = dt/(dy)^2; r3 = dt/(dy)^3;%The ratios r1,r2 and
r3.
for k=1:K-1
    for j=2:N-1
        u(k+1,j)=u(k,j)-vnought*r1/2*(u(k,j+1)-u(k,j-1))-
2*ER*dt*w(k,j)-...
            SQUAREDM*dt/(1+em^2)*(em*w(k,j)+u(k,j))+r2*(u(k,j+1)-
...
            2*u(k,j)+u(k,j-1))+2*kappa^2*(r2/4*y(j)*(u(k,j+1)-...
            u(k,j-1))^2+r3/2*y(j)^2*(u(k,j+1)-u(k,j-1))*(u(k,j+1)-
...
            2*u(k,j)+u(k,j-1)));%Computation of u (secondary
velocity)
        w(k+1,j)=w(k,j)-vnought*r1/2*(w(k,j+1)-w(k,j-
1))+2*ER*dt*u(k,j)+...
            SQUAREDM*dt/(1+em^2)*(em*u(k,j)-
w(k,j))+dt*(GRL*theta(k,j)+...
            GRC*C(k,j))+r2*(w(k,j+1)-2*w(k,j)+w(k,j-1))+...
            2*kappa^2*(r2/4*y(j)*(w(k,j+1)-w(k,j-1))^2+...
            r3/2*y(j)^2*(w(k,j+1)-w(k,j-1))*(w(k,j+1)-...
            2*w(k,j)+w(k,j-1)));%Computation of w (Primary
velocity)
        theta(k+1,j)=theta(k,j)-vnought*r1/2*(theta(k,j+1)-...
            theta(k,j-1))+r2/PR*(theta(k,j+1)-2*theta(k,j)+...
            theta(k,j-1))+EC*r2/4*((u(k,j+1)-u(k,j-
1))^2+(w(k,j+1)-...
            w(k,j-1))^2)+EC*SQUAREDM*dt/(1+em^2)^2*((em*u(k,j)-...
            w(k,j))^2+(em*w(k,j)+u(k,j))^2);%Computation of theta
        C(k+1,j)=C(k,j)-vnought*r1/2*(C(k,j+1)-C(k,j-1))+...
            r2/SC*(C(k,j+1)-2*C(k,j)+C(k,j-1));%Computation of C
    end
end

%OUTPUTS
%
h = 0.2;%Time of observation
tl = h/dt+1;%Corresponding time level

figure (1)%Primary velocity profiles
hold all
plot(y,w(tl,:),'-')
xlabel('$y$','interpreter','latex','FontSize',18,'FontWeight','bol
d')
ylabel('$w(y,t)$','interpreter','latex','FontSize',18,'FontWeight'
,'bold')
title(['Primary Velocity Profiles at  ',sprintf('$t = %g$',h)],...
    'interpreter','latex','FontSize',18)
%title('Primary Velocity Profiles at Various
Times','interpreter',...
    %'latex','FontSize',18)
[~,~,~,current_entries] = legend;
legend([current_entries {sprintf('$Pr =
%g$',PR)}],'interpreter','latex');
       %Effect of Prandtl number, can be changed to other fluid
properties
```

```
117
118   figure (2)%Secondary velocity profiles
119   hold all
120   plot(y,u(tl,:),'-')
121   xlabel('$y$','interpreter','latex','FontSize',18,'FontWeight','bol
122   d')
123   ylabel('$u(y,t)$','interpreter','latex','FontSize',18,'FontWeight'
124   ,'bold')
125   title(['Secondary Velocity Profiles at  ',sprintf('$t =
126   %g$',h)],...
127       'interpreter','latex','FontSize',18)
128   %title('Secondary Velocity Profiles at Various
129   Times','interpreter',...
130       %'latex','FontSize',18)
131   [~,~,~,current_entries] = legend;
132   legend([current_entries {sprintf('$Ec =
133   %g$',EC)}],'interpreter','latex');
134          %Effect of Prandtl number, can be changed to other fluid
135   properties
136
137   figure (3)%Temperature profiles
138   hold all
139   plot(y,theta(tl,:),'-')
140   xlabel('$y$','interpreter','latex','FontSize',18,'FontWeight','bol
141   d')
142   ylabel('$\theta(y,t)$','interpreter','latex','FontSize',18,...
143       'FontWeight','bold')
144   title(['Temperature Profiles at  ',sprintf('$t = %g$',h)],...
145       'interpreter','latex','FontSize',18)
146   %title('Temperature Profiles at Various Times','interpreter',...
147       %'latex','FontSize',18)
148   [~,~,~,current_entries] = legend;
149   legend([current_entries {sprintf('$Pr =
150   %g$',PR)}],'interpreter','latex');
151          %Effect of Prandtl number, can be changed to other fluid
152   properties
153
154   figure (4)%Concentration profiles
155   hold all
156   plot(y,C(tl,:),'-')
157   xlabel('$y$','interpreter','latex','FontSize',18,'FontWeight','bol
158   d')
159   ylabel('$C(y,t)$','interpreter','latex','FontSize',18,'FontWeight'
160   ,'bold')
161   title(['Concentration Profiles at  ',sprintf('$t = %g$',h)],...
162       'interpreter','latex','FontSize',18)
163   %title('Concentration Profiles at Various Times','interpreter',...
164       %'latex','FontSize',18)
165   [~,~,~,current_entries] = legend;
166   legend([current_entries {sprintf('$Pr =
167   %g$',PR)}],'interpreter','latex');
168          %Effect of Prandtl number, can be changed to other fluid
169   properties
170   %}
171   %{
172   figure (5)%3-D Mesh for primary velocity
173   clear figure
174   mesh(y,t,w)
175   xlabel('$y$','interpreter','latex','FontSize',18)
176   ylabel('$t$','interpreter','latex','FontSize',18)
177   zlabel('$w(y,t)$','interpreter','latex','FontSize',18)
```

```
178   title(['Primary velocity ',sprintf('$3-D$'),' Mesh
179   Plot'],'interpreter',...
180       'latex','FontSize',18)
181   %}
182   %{
183   figure (6)%3-D Mesh for secondary velocity
184   clear figure
185   mesh(y,t,u)
186   xlabel('$y$','interpreter','latex','FontSize',18)
187   ylabel('$t$','interpreter','latex','FontSize',18)
188   zlabel('$u(y,t)$','interpreter','latex','FontSize',18)
189   title(['Secondary velocity ',sprintf('$3-D$'),' Mesh Plot'],...
190       'interpreter','latex','FontSize',18)
191   %}
192   %{
193   figure (7)%3-D Mesh for temperature
194   clear figure
195   mesh(y,t,theta)
196   xlabel('$y$','interpreter','latex','FontSize',18)
197   ylabel('$t$','interpreter','latex','FontSize',18)
198   zlabel('$\theta(y,t)$','interpreter','latex','FontSize',18)
199   title(['Temperature ',sprintf('$3-D$'),' Mesh
200   Plot'],'interpreter',...
201       'latex','FontSize',18)
202   %}
203   %{
204   figure (8)%3-D Mesh for concentration
205   clear figure
206   mesh(y,t,C)
207   xlabel('$y$','interpreter','latex','FontSize',18)
208   ylabel('$t$','interpreter','latex','FontSize',18)
209   zlabel('$C(y,t)$','interpreter','latex','FontSize',18)
210   title('Concentration 3D Mesh
211   Plot','interpreter','latex','FontSize',18)
212   %}
213   %{
214   figure (9)%Initial value subplots
215   subplot (1,3,1)
216   plot(y,w(1,:),'-')
217   xlabel(texlabel('y'),'FontSize',12, 'FontWeight','bold')
218   ylabel(texlabel('w(y,0)'),'FontSize',12, 'FontWeight','bold')
219   title('Initial Primary Velocity Profile')
220   subplot (1,3,2)
221   plot(y,theta(1,:),'-')
222   xlabel(texlabel('y'),'FontSize',12, 'FontWeight','bold')
223   ylabel(texlabel('theta(y,0)'),'FontSize',12, 'FontWeight','bold')
224   title('Initial Temperature Profile')
225   subplot (1,3,3)
226   plot(y,C(1,:),'-')
227   xlabel(texlabel('y'),'FontSize',12, 'FontWeight','bold')
228   ylabel(texlabel('C(y,0)'),'FontSize',12, 'FontWeight','bold')
229   title('Initial Concentration Profile')
230   %}
231   end
```